Assessment of Respiratory Flow and Efforts Using Upper-Body Acceleration Considering Sleep Apnea Syndrome

by

Parastoo Kheirkhah Dehkordi

M.Sc., Azad University of Tehran, 2003
B.Sc., University of Esfahan, 2000

Thesis Submitted in Partial Fulfillment
of the Requirements for the Degree of
Master of Applied Science

In the
Engineering Science Department
Faculty of Applied Sciences

SIMON FRASER UNIVERSITY

Summer 2012

Approval

Name: **Parastoo Kheirkhah Dehkordi**

Degree: **Master of Science**

Title of Thesis: ***Assessment of Respiratory Flow and Efforts Using Upper-Body Accelerations Considering Sleep Apnea Syndrome***

Examining Committee:

Chair: Dr. John Jones
Assistant Professor

Dr. Bozena Kaminska
Senior Supervisor
Professor

Dr. Carlo Menon
Supervisor
Assistant Professor

Dr. Andrew Rawicz
Internal Examiner
Professor
School of Engineering Science

Date Defended/Approved: May 31, 2012

Partial Copyright Licence

Abstract

Sleep apnea monitoring requires measurement of both the respiratory flow and efforts in order to detect apnea periods and classify them into obstructive and central ones. In this thesis, an innovative method for estimating the respiratory flow and efforts is proposed and validated in various sleeping postures and flow rates. Three MEMS accelerometers were mounted on the suprasternal notch, thorax and abdomen of the subjects in supine, prone and lateral positions to record the upper airway acceleration and the chest and abdomen walls movement. The respiratory flow and efforts are estimated from the recorded acceleration signals by applying system identification techniques. To assess the agreement of estimated signals with the well-established measurement methods, Standard Error of Measurement (SEM) was calculated and ρ=1-SEM was derived from it for every condition. Additionally, t_{PTEF}/t_E and t_{PTIF}/t_I ratios for each breathing cycle of the estimated and the reference flow were calculated.

Keywords: obstructive sleep apnea; central sleep apnea; Polysomnography (PSG); Machine learning methods

To Parnian and Parmin,
instead of all lullabies and bed time stories.

To Nick,
for his patience and kindness

Acknowledgements

To my supervisor, Dr. Bozena Kaminska, who gave me the wings to fly. I offer my endless gratitude for her understanding, leadership and support for my works. And thanks for all her inspiration as a successful senior researcher and a brilliant mother.

Many thanks to Dr. Carlo Menon for his help and input.

Special thanks to Dr. Kouhyar Tavakolian as he made available his support in a number of different ways to this research during the last two years. I definitely would not been able to finish this work without his help and support.

Many thanks to Dr. Marcin Marzencki for all support, help and motivation he brought to this project.

It is an honour for me that I have had the consultation and inspirations of a knowledgeable respiratory specialist in this study, Dr. Marta Kaminska, from whom I have learnt a lot about the respiration and sleep apnea syndrome.

To Dr. Rodney Vaughan, with his lessons I started signal processing.

Also I offer my regards and blessings to my friends and colleagues for their support, motivation and inspiration: Maryam Dehghani and Farzad Khosrow-khavar.

Special thanks to all my colleagues at SFU and CiBER lab.

And finally I am eternal grateful to Nick Langroudi for his unwavering patience, trust and support.

Table of Contents

List of Tables

List of Figures

Glossary

OSA	Obstructive Sleep Apnea
AHI	Apnea/Hypopnea Index
OSAHS	Obstructive Sleep Apnea Hypopnea Syndrome
CSA	Central Sleep Apnea
CSR	Cheyne-Stokes Respiration
EDR	ECG Derived Respiratory
ADR	Accelerometer Derived Respiratory
PSG	Polysomnography
HST	Home Sleep Test
SEM	Standard Error Measurement
PTIF	peak tidal inspiratory flow
PTEF	peak tidal expiratory flow
t_{PTIF}	time to peak tidal inspiratory flow
t_{PTEF}	time to peak tidal expiratory flow
SIDS	Sudden Infant Death Syndrome
RIP	Respiratory Inductance Plethysmography
F_{nasal}	Reference flow recorded by nasal/oral cannula connected to the pressure transducer
F_{est}	Estimated flow
V_{Th}	Reference thoracic respiratory effort recorded by strain gauge transducer mounted on belt
E_{Th}	Estimated thoracic respiratory effort
V_{Abd}	Reference abdominal respiratory effort recorded by strain gauge transducer mounted on belt
E_{Abd}	Estimated abdominal respiratory effort

1. Introduction and Motivations

Sleep apnea described by repetitive cessations of breathing during sleep is a significant sleep breathing disorder. Sleep apnea is classified into three types: obstructive, central and mixed. Obstructive sleep apnea (OSA) is characterized by partial or complete interruption of airflow to the lungs caused by collapse of upper airway (Malhotra & White 2002). Central sleep apnea occurs when there is lack of drive to the muscles responsible for inducing breath during sleep (Malhotra & Owens 2010). In contrast to the obstructive sleep apnea, in which ongoing respiratory efforts are observed, the central apnea is defined by lack of respiratory effort during the cessations of airflow (Malhotra & White 2002). Since the two types of sleep apnea need different types of treatment, classifying the apnea periods into obstructive and central cessations is of great interest. Thus, monitoring of upper airway flow is necessary for detecting apnea periods and screening of the respiratory efforts is essential to classify these periods into obstructive or central ones.

Overnight, laboratory-based polysomnography (PSG) is the most commonly used test for diagnosing sleep breathing disorder such as sleep apnea and also determining the severity of disorder. PSG, known as sleep test, is a comprehensive multi parametric test which monitors the several biophysiological changes during sleep. However for detecting sleep apnea, monitoring the respiratory flow, the respiratory efforts and the changes of oxygen levels in blood are mandatory (Randerath, Sanner, & Somers 2006).

Respiratory flow is measured with a nasal/oral cannula fitted near the nostrils and connoted to pressure transducer. This allows measuring breathing rate and also monitoring the breathing cessation. Respiratory efforts are considered as thoracic and abdominal movement due to respiration and measured by the use of two belts fastened around the chest and abdomen of patient. The belts typically use piezoelectric sensors or respiratory inductance plethysmography (RIP) techniques. Changes in blood oxygen level that often happen with sleep apnea is measured by the pulse oximetry fitted over a finger tip or an ear lobe.

Sleep apnea is common sleep breathing disorder worldwide and in North America, estimated to affect at least three percent of the adult population (Young, Peppard, & Gottlieb, 2002). According to the public health agency of Canada (public health agency of Canada, 2007), sleep apnea in Canada is as populated as in other developed countries. Patient which are suspected for sleep apnea are referred to sleep lab for PSG test. PSG is an overnight complex test which is performed at a special sleep center by a specially trained technologist under supervision of a qualified physician who later interprets the recorded results. Due to the paucity of sleep labs and long waiting list, the referred patients need to wait for a long time from 4 weeks to 6 months to be scheduled for PSG (Coren, 1996). In addition the overnight PSG is an expensive diagnosis test for sleep apnea. Simplified testing at home is possible for selected patients (Chesson, Berry, & Pack, 2003) but uses the same basic techniques as PSG. The complex set-up required for sleep testing may affect sleep architecture, resulting in inaccurate results. Therefore, a significant number of apnea cases remain under diagnosed; a situation that leads to a considerable interest in development of reliable and simple low cost techniques for the identification of individuals with sleep breathing disorders.

In this line, during the recent years, many investigators have started the considerable search to find the extremely simple systems for diagnosing sleep apnea. These systems have to be easy for handling to be used at home and very simple regarding with application to be used by non-expert person. Portable devices are remarkable examples of these systems (Chesson, Berry, & Pack, 2003).

Since the sleep apnea is a respiratory disorder, the simple solution to detect sleep apnea periods and distinguish between them should record at least respiratory airflow and efforts signals.

In this study, we proposed a method to estimate the upper airway flow and the respiratory efforts using three tri-axial MEMS accelerometers placed on the upper-body. The three accelerometers were mounted on:

1. The suprasternal notch to monitor the airflow in upper airway indirectly that consequently allows for indirect detection of breathing cessation.

2. The left seventh rib interspace to monitor the movement of rib case due to respiratory that allows for indirect measuring of thorax respiratory efforts
3. And on the abdomen to monitor the movement of abdomen wall for measurement of abdominal respiratory efforts.

The machine learning techniques were adopted to estimate the respiratory activities from recorded signals. To assess the agreement, we compared the estimated flow to the oronasal flow signal picked up by a nasal/oral cannula and compared the estimated respiratory efforts to the readings obtained with two strain gauge belts.

Synopis

Chapter 2 of this thesis provides background information on sleep apnea syndrome, its historical diagnosis and also new approaches to detect this breathing disorder. Reviewing machine learning and ensemble learning methodologies are presented in this chapter too.

The materials and methods are explained in chapter 3. In 3.1 we discussed about participants who took placed in data acquisition process, list of materials used for signal recording and also data recording protocol and procedure. In 3.2, the methods for estimating respiratory flow and efforts were described briefly. Assessment the agreement between estimated and reference signals are presented in 3.3.

Chapter 4 details the results of apply the proposed method in chapter three on recorded data. The discussion about the results takes place at the end of this chapter.

Chapter 5 concludes the thesis with the look at future works and also the limitations of proposed method.

2. Literature review and background

2.1. General features of respiration

Respiration refers to the entire process involved in the exchange of O_2 and CO_2 between the environment and the cells of the body. Ventilation (Breathing) as a part of respiration refers to the exchange of air between the lungs and the environment.

Ventilation is also defined as the rate at which air is moved into the lungs. When the utilization of O_2 and the production of CO_2 vary, the respiratory system must respond to these variations. One mechanism is available which operates during rest and sleep referred to as *chemical control of ventilation*. This system monitors the blood level of O_2 and CO_2 and varies the level of ventilation in response to deviation in the levels of these blood gases (Batzel, Kappel, Schneditz, & Tran, 2007). The mechanism for controlling the ventilation during the exercise or voluntary changes ventilation is not well understood and still under active investigation.

A single breath involves inspiration and expiration.

The inspiration is the more active process although it also contains the passive mechanical properties of airways, lungs and chest. Inspiration takes up about 35-40% of the time of a breath (Stocks, Sly, Tepper, & Morgan, 1996).

The respiratory flow is defined as the speed of the air can be inhaled and exhaled.

A breathing pattern measured during tidal (regular) breathing contains significant physiological information about respiratory function. The most fundamental parameters contained in the flow and volume signals are shown in Figure 1 and defined as follow (Bates, Schmalisch, & Stocks, 2000) :

- **Respiratory frequency (f_R):** the respiratory frequency or rate is the number of breaths that occur in a minute.
- **Tidal volume (V_T):** the normal volume of air displaced between normal inspiration and expiration during tidal breathing.
- **Inspiratory time (t_I):** Taken from a flow waveform, it is the time in seconds from the zero flow at the end of the expiratory phase of the preceding breath to the next zero point of flow at the end of inspiration.
- **Expiratory time (tE**): Taken from a flow waveform, it is the time in seconds from the zero flow at the end of the inspiratory phase to the next zero point of flow at the end of expiration.
- **Total breathing time (t_{tot}):** From a flow waveform, it is the time in seconds from the point of zero flow immediately prior to the onset of the inspiration of one breath to the point of the zero flow immediately prior to the onset of the inspiration of the next breath.
- **Time to peak tidal expiratory flow (t_{PTEF}):** time from the onset of expiration to the peak expiratory flow.
- **Time to peak tidal inspiratory flow (t_{PTIF}):** time from the onset of inspiration to the peak inspiratory flow.

These basic parameters can be used to calculate other parameters related to the more detailed aspects of the breathing patterns such as:

- **t_{PTIF}/t_I :** Ratio of time at the tidal peak inspiratory flow to the inspiratory time
- **t_{PTEF}/t_E :** Ratio of time at the tidal peak expiratory flow to the expiratory time

Inspiratory flow measurement is more important for evaluation of disorder like obstructive sleep apnea where the limitation is in upper airway above the thoracic inlet (Ent & Grinten, 1998). Ratio of time at the tidal peak inspiratory flow to the inspiratory time (t_{PTIF}/t_I) is one of parameters used for observing inspiratory flow.

Expiratory flow measurement is important for the assessment of disorders like asthma, where the obstruction is intra-thoracic and therefore apparent on expiration. The ratio t_{PTEF}/t_E is used to detect airflow obstruction especially in young children and to monitor the reduced lung function early in life (Ent & Grinten, 1998).

Obtaining tidal breathing parameters requires nothing more than the measurement of flow or volume at the mouth or nose during a period of regular breathing.

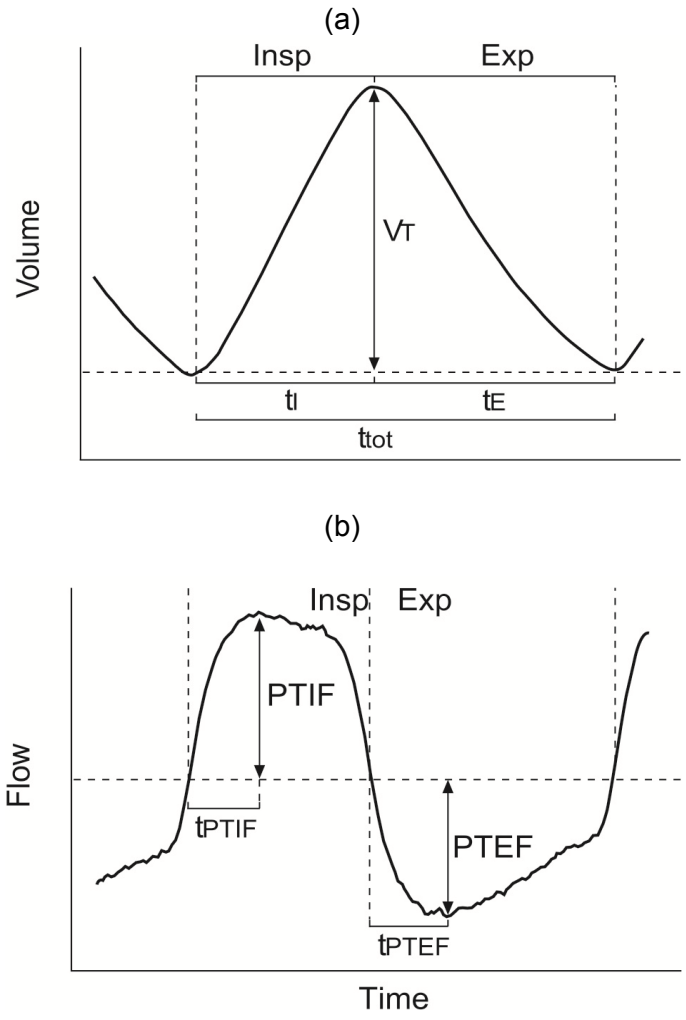

Figure 1. ***Tidal breathing parameters of the flow: a) Flow signal. b) Volume signal. Insp: inspiration; exp: expiration; PTIF:peak tidal inspiratory flow;PTEF: peak tidal expiratory flow;tPTIF: time to peak tidal inspiratory flow; tPTEF: time to peak tidal expiratory flow (Bates, Schmalisch, & Stocks, 2000)***

2.2. Sleep breathing disorders

Sleep breathing disorders are a group of disorders that affect the breathing while the person is asleep and are characterized by disruptions of normal breathing patterns during sleep.

Classification of sleep breathing disorders has been suggested in 1999 by the American Academy of Sleep Medicine (AASM) and has been confirmed through 2nd International Classification of Sleep Disorders (ICSD II), published in 2005 (American Academy of Sleep Medicine, 2005). This classification basically includes four different categories:

- Obstructive Sleep Apnea/Hypopnea Syndrome(OSAHS),
- Central Sleep Apnea Syndrome (CSA),
- Central sleep apnea syndrome with Cheyne-Stokes respiration,
- Obesity hypoventilation syndrome.

Obstructive and central sleep apnea syndromes are extensively presented in this thesis while there are few details about two latter.

2.2.1. *Obstructive Sleep Apnea/Hypopnea Syndrome*

Definition

Sleep apnea is defined as the cessation of airflow for at least 10s during sleep. It is also characterized by reduction in flow to 30% of normal breathing. Sleep apnea is associated by at least a 4% drop in oxygen in the blood which is a direct result of the reduction in the transfer of oxygen into the blood when breathing stops (Malhotra & White, 2002).

Hypopnea is characterized by a reduction in airflow as a 69% to 26% of a normal breath. Like apneas, hypopneas also may be defined as a 4% or greater drop in oxygen in the blood (Nabili & Verneuil, 2004).

Obstructive Sleep Apnea/Hypopnea (OSAH) is defined as the apnea/hypopnea caused by complete or partial pharyngeal collapse associated with total or partial absence of airflow during sleep.

In both obstructive apnea and hypopnea, respiratory effort, movement of chest and abdomen walls is present during respiratory cessations.

Figure 2 illustrated the segments of recorded flow signal, thorax and abdominal effort signals and O_2 level signal respectively from top to bottom. In this figure the periods of obstructive sleep apnea with the cessation of airflow due to the upper airway collapse are annotated. The thoracic and abdominal respiratory efforts are present. The periods of oxygen desaturation are also highlighted in this figure.

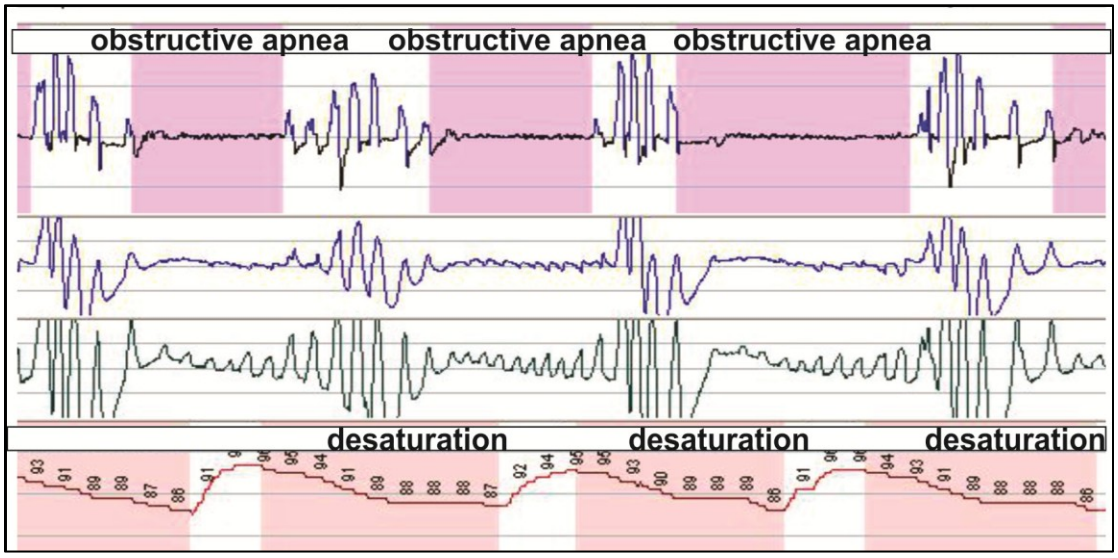

Figure 2. ***Obstructive sleep apnea with cessation of airflow due to upper airway obstruction despite the presence of respiratory efforts. From top to bottom: flow signal, thoracic and abdominal signals and variations in blood oxygen level.***

Note. The figure was annotated by Dr. Marta Kaminska and reproduced with her permission for this thesis.

Figure 3 illustrates the periods of hypopnea with the reduction in airflow and the presence of the thoracic and abdominal efforts. The periods of oxygen desaturation are highlighted in this figure too.

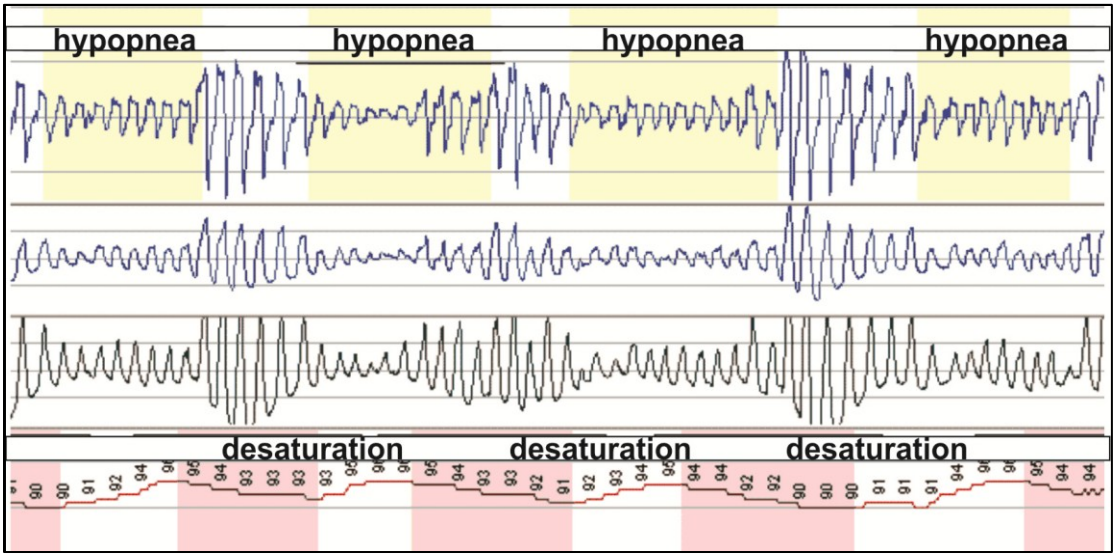

Figure 3. ***Hypopnea with reduction in airflow due to upper airway partial collapse despite the presence of respiratory efforts. From top to bottom: flow signal, thorax and abdominal signals and variations in blood oxygen level.***

Note. The figure was annotated by Dr. Marta Kaminska and reproduced with her permission for this thesis.

Severity of obstructive sleep apnea/hypopnea is measured as Apnea/ Hypopnea Index (AHI). AHI is defined as the number of Apnea/ Hypopnea periods in one hour. Using American Academy of Sleep Medicine definition , if these respiratory events happen more than 10 times per hour and be associated with snoring and excessive daytime fatigue the term Obstructive Sleep Apnea/Hypopnea Syndrome (OSAHS) is applied. OSAHS may be classified into three categories in term of severity (Nabili & Verneuil, 2004):

- ***Mild OSAHS*** with 5-15 apneas/hypopneas per hour
- ***Moderate OSAHS*** with15-30 apneas/hypopneas per hour
- ***Severe OSAHS*** with more than 30 apneas/hypopneas per hours

Pathophysiology

Through an open upper airway, air goes forward from the nose and/or mouth to the lungs. In fact, the stability of upper airway is essential for breathing. This stability depends upon the anatomy and function of pharynx. The collapse of the upper airway takes place by negative pressure within the airway during inspiration and positive pressure outside the airway. Figure 4 shows the unblocked airway in normal sleep breathing vs. the blocked airway in obstructive sleep apnea.

Both inspiration and expiration require changes in the pressure within the thoracic cavity which is done by the aid of the various muscles of respiration (Malhotra & White, 2002). During the inhalation, the rib cage expands and the diaphragm contracts, expanding the chest cavity. This causes the pressure in the chest cavity to decrease, and the lungs expand to fill the space. This, in turn, causes the pressure of the air inside the lungs to decrease (it becomes negative, relative to the atmosphere), and air flows into the lungs from the atmosphere. In normal breathing, inspiratory muscles are activated downwards in a progressive and controlled form. In this way, pharyngeal muscles will be already contracted when submitted to the airway negative pressure. A peak of muscular pharyngeal activity happens before the muscular thoracic activity. If there is any incoordination in the intensity or timing of pharyngeal muscular activity with respect to the thoracic one, the upper airway may collapse (Malhotra & White, 2002).

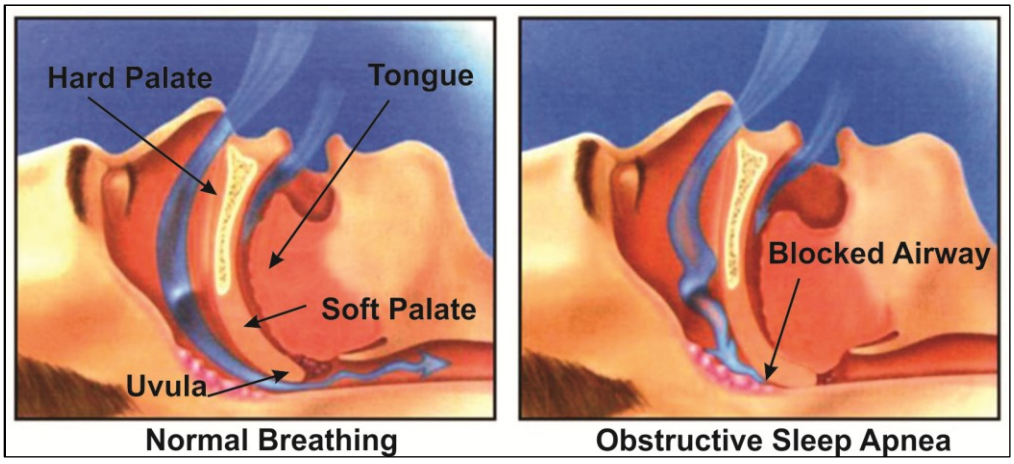

Figure 4. ***Unblocked airway in normal sleep breathing vs. blocked airway in obstructive sleep apnea***

There is the variety range of factors that may results in collapsing upper airway. Some structural factors including undersized jaws, Inferior displacement of the lingual bone or high arched palate predispose patients with obstructive sleep apnea. Nonstructural risk factors for OSA include the following (Nabili & Verneuil, 2004):

- Obesity
- Central fat distribution
- Male sex
- Age
- Postmenopausal state
- Alcohol use
- Sedative use
- Smoking
- Habitual snoring with daytime somnolence
- Supine sleep position
- Rapid eye movement (REM) sleep

During sleep in patients with OSAHS, the occurrence of apneas or hypopneas is most common in stages 1 and 2 of NREM and in REM sleep (Randerath, Sanner, & Somers, 2006). Pharynx collapsibility increases with sleep fragmentation and with mouth opening during sleep (Randerath, Sanner, & Somers, 2006)

Consequence

In obstructive sleep apnea (OSA), when an apnea or hypopnea occurs, sleep usually is disrupted due to inadequate breathing and poor oxygen levels in the blood. Figure 5 shows the cycle of airway collapse and arousal during sleep obstructive apnea/hypopnea. This cycle have four components:

1. First, the airway collapses or becomes obstructed.
2. Second, an effort is made to take a breath, but it is unsuccessful.
3. Third, the oxygen level in the blood drops as a result of unsuccessful breathing.
4. Finally, when the amount of oxygen reaching the brain decreases, the brain signals the body to wake up and take a breath.

The consequences of repetitive arousals are well established and include sleepiness, day time fatigue, lengthened reaction times, reduced creativity, decreased quality of life, and increased accidents (Randerath, Sanner, & Somers, 2006).

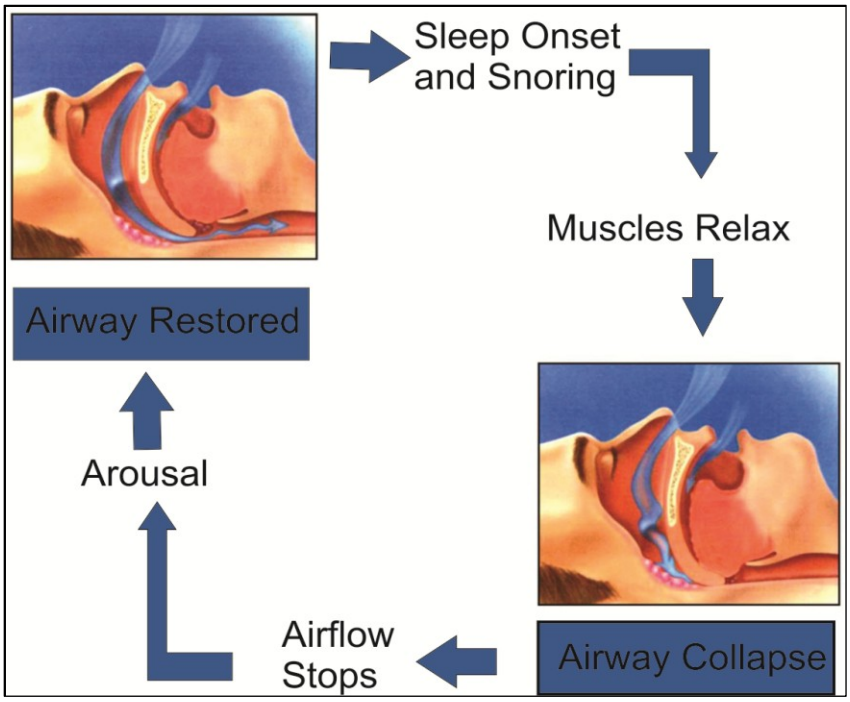

Figure 5. The cycle of obstructive sleep apnea

The other complications of obstructive sleep apnea include high blood pressure, strokes, congestive heart failure as well as difficulties in concentrating, thinking and remembering. In some cases obstructive sleep apnea may leads to sudden death.

Prevalence

A study by Young and colleagues (Young, Peppard, & Gottlieb, 2002) showed that 4% of men and 2% of women in a middle-aged North American population had symptoms of moderate to severe obstructive sleep apnoea.

According to Public Health Agency of Canada (Public Health Agency of Canada, 2007), there is a lack of information on the Canadian prevalence of sleep disordered breathing. Population studies suggest that sleep disordered breathing is at least as prevalent in Canada as in other industrialized nations.

2.2.2. *Central Sleep Apnea*

Definition

Central sleep apnea (CSA) is defined by a lack of drive to breathe during sleep, resulting in insufficient or absent ventilation (Malhotra & Owens, 2010). In contrast to obstructive sleep apnea (OSA), in which ongoing respiratory efforts are present, central apnea is associated by the lack of respiratory effort during cessations of airflow.

Figure 6 shows the segments of recorded flow signal, thorax and abdominal effort signals and O_2 level signal respectively from top to bottom. The figure highlights the periods of central apnea with cessation in airflow and the absence of the thorax and abdominal respiratory efforts. The periods of oxygen desaturation, a direct result of the reduction in the transfer of oxygen into the blood when breathing stops, are also annotated in this figure.

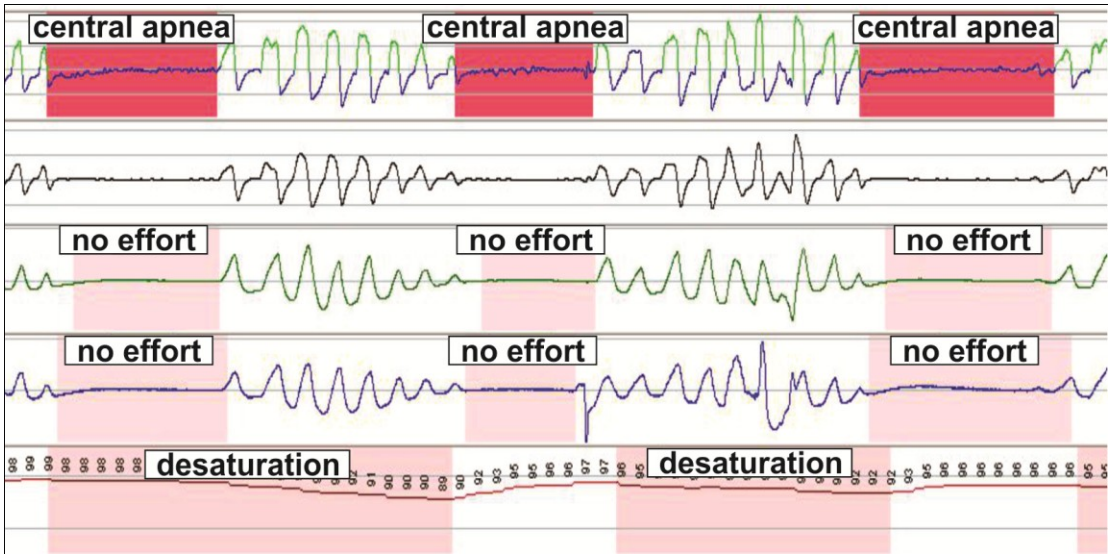

Figure 6. ***Periods of central apnea with cessation in airflow and the absence of efforts. From top to bottom: flow signal, thorax and abdominal signals and variations in blood oxygen level.***

Note. The figure was annotated by Dr. Marta Kaminska and reproduced with her permission for this thesis.

Pathophysiology

In respiratory medicine, minute ventilation is defined as the volume of gas inhaled to or exhaled from a person's lungs in one minute (Randerath, Sanner, & Somers, 2006). Partial pressure of CO_2 in blood (P_{CO2}) determines the minute ventilation. During wakefulness the P_{CO2} is tightly maintained near 40 mmHg. However, during sleep the chemosensitivity of CO_2 and O_2 fall. P_{CO2} increases to 45 mmHg during stable sleep, causes the reduction in minute ventilation (Randerath, Sanner, & Somers, 2006).

In normal respiratory after exhalation, P_{CO2} increases. Exchange of gases with a lungful of fresh air is necessary to get oxygen again and rid the bloodstream of carbon dioxide. Oxygen and carbon dioxide chemoreceptors in the bloodstream send nerve impulses to the brain, which then signals reflex opening of the larynx and movements of the rib cage muscles and diaphragm. These muscles expand the thorax so that a negative pressure is made within the lungs and air rushes in to fill them (Randerath, Sanner, & Somers, 2006).

During central apneas, the central respiratory drive is absent and the brain does not respond to changing blood levels of the respiratory gases. No breath is taken despite the normal signals to inhale.

Consequence

CSA, like OSA, is associated with important complications, including sleepiness and excessive daytime fatigue.

The immediate effects of central sleep apnea on the body depend on how long the failure to breathe lasts. At worst, central sleep apnea may cause to death (Malhotra & Owens, 2010).

Prevalence

Central sleep apnea is relatively uncommon, but it is quite common in patients with cardiac or neurological disease. One study (Javaheri, Parker, & Wexler, 1995) suggests that 45% of patients with congestive heart failure suffering from central sleep apnea too.

Mixed sleep apnea

Mixed sleep apnea, occurs when there is both central sleep apnea and obstructive sleep apnea/hypopnea (Nabili & Verneuil, 2004). When obstructive sleep apnea syndrome is severe and longstanding, episodes of central apnea sometimes develop.

Figure 7 shows the periods of obstructive apnea, obstructive hypopnea and central apnea that happened together. This breathing pattern is also associated with oxygen desatuation.

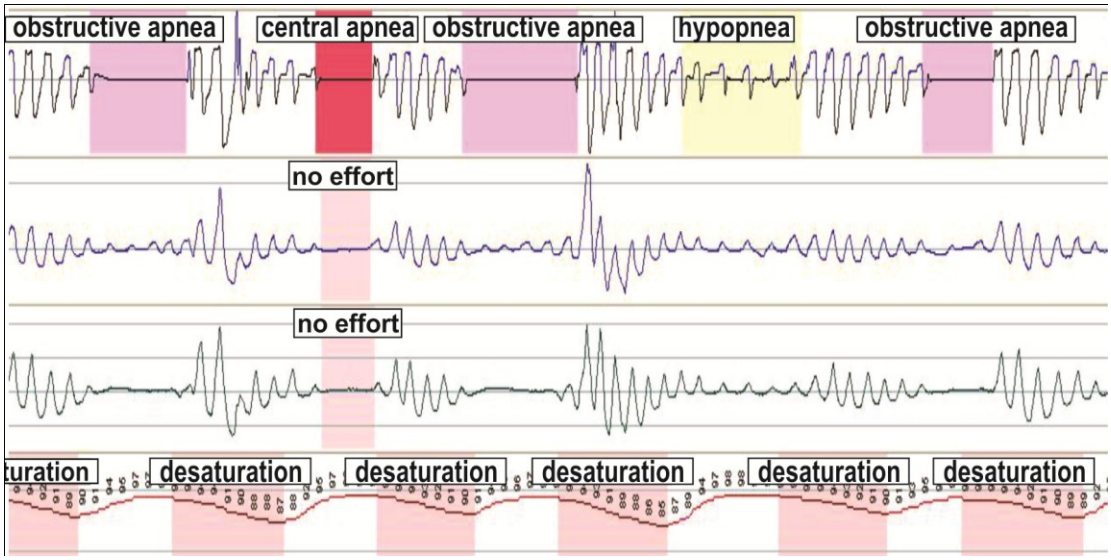

Figure 7. ***The periods of obstructive apnea, obstructive hypopnea and central apnea happened together. From top to bottom: flow signal, thorax and abdominal signals and variations in blood oxygen level.***

Note. The figure was annotated by Dr. Marta Kaminska and reproduced with her permission for this thesis.

2.2.3. *Central sleep apnea syndrome with Cheyne - Stokes respiration*

This is a condition including both central apneas and hypopneas and Cheyne-Stokes respiration (CSR). Cheyne-Stokes respiration (CSR) is an abnormal pattern of breathing characterized by progressively deeper and sometimes faster breathing, followed by a gradual decrease that results in a temporary stop in breathing (apnea)

(Malhotra & Owens, 2010). The pattern repeats, with each cycle usually taking 30 seconds to 2 minutes.

Figure 8 depicts the pattern Cheyne-Stokes breathing with central apnea periods.

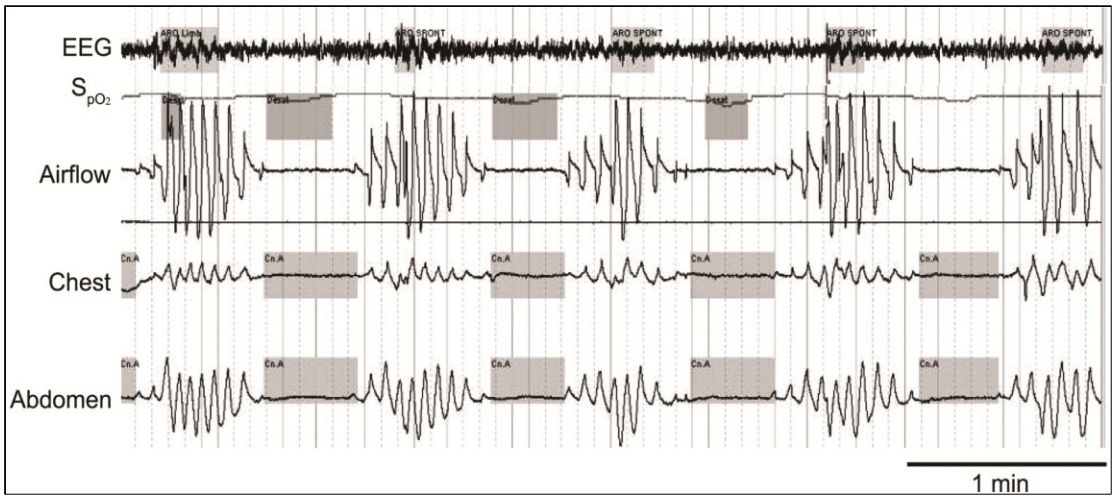

Figure 8. ***Central apnea with Cheyne-Stokes breathing pattern with the periods of deep and fast breathing followed by cessation of breathing (Malhotra & Owens, 2010)***

2.2.4. *Obesity Hypoventilation Syndrome*

This is a condition in which there is both obesity and hypercapnia (Randerath, Sanner, & Somers, 2006). Hypercapnia is defined as the condition where there is the large amount of CO_2 in the bloodstream. There is possibly either hypoventilation or apneas or both during sleep. As obesity is more and more epidemic worldwide, obesity hypoventilation syndrome is a rapidly growing.

2.3. Measuring respiration

Precise monitoring of respiratory flow and effort is of great interest in detection of sleep breathing disorders such as Obstructive Sleep Apnea/Hypopnea (OSA/H) or Central Sleep Apnea (CSA). This section has the brief introduction to the techniques used in measuring respiratory flow and effort.

2.3.1. *Measuring respiratory flow*

The respiratory flow is defined as the speed of the air can be inhaled and exhaled. Measuring the respiratory flow is usually achieved by spiromety devices such as pneumotachographer or a nasal/oral cannula connected to the pressure transduceror.

Pneumotachographer

Although there are several different types of pneumotachographer, the test process is the same for all of them. During the test, the patient would be asked to breathe through a mouthpiece while wearing a nose clip. Although using the pneumotachographer is the most accurate method for measuring flow (Tarrant, Ellis, Flack, & Selley, 1997), it changes the breathing pattern (Gilbert, Auchincloss, Brodsky, & Boden, 1972) and cannot be used for continuous monitoring of airflow.

Figure 9(a) shows a type of spirometry device used in the hospitals and respiratory clinics for monitoring respiratory flow.

Figure 9(b) depicts SPR-BTA spirometer (Vernier Software & Technology,Beaverton, OR). This small spirometry device designed to measure human respiratory at rest and during moderate activity was used in CiBER lab to measure airflow during respiratory recording experiments.

Nasal/oral cannula connected to a pressure transducer

A medical device made of plastic tubing that is utilized to deliver supplemental airflow or oxygen to a person who requires respiratory assistance is called a nasal cannula.

A nasal cannula connected to a pressure transducer can use to measure the air flow during respiration (Rapoport, Norman, & Nielson, 2001). Nasal cannula pressure systems generate the airflow waveform signal by detecting the fluctuations in pressure caused by inspiration and expiration.

Figure 10 shows the nasal cannula (Model 0589, Braebon Canada, Kanata, ON) used in this study and the way to wear that.

(a) (b)

Figure 9. ***(a) Device into which a patient breathes for Spirometry. Photographed at Swedish Hospital Ballard Campus, Seattle, Washington. (b) The spirometer designed to measure human respiratory at rest and during moderate activity. Used in CiBER***

(a) (b)

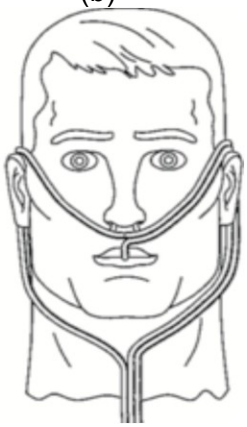

Figure 10. ***(a) The type of nasal cannula used in this study (Model 0589, Braebon Canada, Kanata, ON). (b) how to wear the nasal cannula***

Figure 11 shows the type of pressure transducer (Model 0585, Braebon Canada, Kanata, ON) used for measuring respiratory flow for this study in CiBER lab.

Figure 11. The type of pressure transducer used in this study (Model 0585, Braebon Canada, Kanata, ON)

2.3.2. *Measuring respiratory effort*

Respiratory effort -effort to breathe- is defined as the esophageal pressure during respiration. Respiratory effort is directly measured by esophageal manometry. During esophageal manometry, a thin, pressure-sensitive tube is passed through the patient's mouth or nose and into the stomach. Once in place, the tube is pulled slowly back into the patient's esophagus.When the tube is in patient's esophagus, the patient will be asked to swallow. The pressure of the muscle contractions will be measured along several sections of the tube. Although esophageal pressure recording is regarded as a gold standard, it is an invasive method and some patients undergoing full polysomnography do not accept the esophageal catheter (Mazeika & Swanson, 2007) .

A reasonable surrogate measure of respiratory effort can be obtained by measuring changes in chest and/or abdominal volume, also known as plethysmography. There are three primary methods of non-invasive chest and abdominal plethysmography (measurement of change in volume) in current use:

- Measurement of changes in elastic belt tension,
- Measurement of changes in electrical impedance,
- And measurement of changes in electrical inductance.

Elastomeric plethysmography

An elastic belt fastened around the chest or abdomen will exhibit a change in tension as the chest or abdomen expands or contracts. This change in tension can be easily measured and converted to a voltage by a variety of methods. The most common method in current use is a piezo-electric sensor, i.e., a crystal that directly generates a voltage when compressed or stretched. This method, while simple and inexpensive, is subject to trapping artifact: it is fairly easy to imagine how a portion of elastic belt may become “trapped” as a person turns from one side to another, resulting in variable tension along the belt circumference. Thus this method can both significantly under and/or overestimate the actual degree of chest or abdominal movement in addition to creating a false signal when belt tension suddenly changes with a change in body position (Mazeika & Swanson, 2007).

Figure 12 shows the respiratory effort transducer (Model SS5LB, BioPac Systems Inc, Camino Goleta, CA) used for recording respiratory efforts during data recording experiments in this study.

Figure 12. The respiratory effort transducer used for data recording in this study

Impedance plethysmography (Malmivou & Plonsey, 1995)

The human body is a fairly poor conductor of electricity. In other words, it presents high impedance to electrical current flowing through it. This impedance changes as the cross-section of the body expands and contracts which allows qualitative measurement of thoracic and abdominal movement during breathing. Two (or sometimes four or more) electrodes are attached to the skin. A weak alternating electrical current is passed through these electrodes, allowing the impedance to be measured. This method yields a non-linear signal, thus is useful only as a qualitative measure of chest or abdominal movement. Given that an electrical current must be passed through the body, care must be taken to choose a frequency range that would not interfere with other monitoring equipment or with implanted equipment such as pacemakers or defibrillators.

Respiratory Inductance Plethysmography (RIP)

RIP is the gold standard for measuring effort. It relies on the principle that a current applied through a loop of wire generates a magnetic field normal to the orientation of the loop (Faraday's Law) and that a change in the area enclosed by the loop creates an opposing current within the loop directly proportional to the change in the area (Lenz's Law).

An elastic belt into which a zigzagging (coiled) wire is sewn (to allow for expansion and contraction) is worn around the chest or abdomen. An alternating current (AC) is passed through the belt, generating a magnetic field. The frequency of the alternating current is set to be more than twice the typical respiratory rate in order to achieve adequate sampling of the respiratory effort waveform. The act of breathing changes the cross-sectional area of the patient's body, and thus changes the shape of the magnetic field generated by the belt, "inducing" an opposing current that can be measured, most easily as a change in the frequency of the applied current.

With RIP, no electrical current passes through the body (a weak magnetic field is present that does not affect the patient or any surrounding equipment). The signal produced is linear and is a fairly accurate representation of the change in cross-sectional area. In addition, RIP does not rely on belt tension, thus is not affected by belt trapping .

2.4. Historical Diagnosis of sleep apnea

In a systematic revision of literature (American Thoracic Society, 2004), the types of monitoring devices for screening sleep apnea were classified into four categories as described following:

Type I: This category includes standard attending in-laboratory polysomnography.

Type II: Type II monitors have a minimum of 7 channels (brain wave (EEG), eye movement (EOG), muscle activities (EMG), heart rate, airflow, respiratory effort and oxygen saturation). This type of device monitors sleep staging in addition to allowing calculation of AHI.

Type III: Type III monitors are limited channel devices (usually 4-7 channels). They have a minimum of 4 monitored channels, including ventilation or airflow (at least 2 channels of respiratory movement or respiratory movement and airflow), heart rate, and oxygen saturation.

Type IV: Type IV devices measure only 1 or 2 parameters (e.g., oxygen saturation or airflow). They typically include oximetry, but not oximetry alone. This changed, however, after the Centers for Medicare and Medicaid Services (CMS) decided to cover continuous positive airway pressure (CPAP) treatment for positive tests from Type IV devices with at least 3 channels (McNicholas & Lévy, 2011)

2.4.1. *Polysomnography*

Polysomnography, abbreviated PSG, known as a sleep study is used to diagnose many types sleep disorders. It is a multi-parametric test which records the biophysiological changes during sleep usually at night.

The PSG monitors many body functions including brain activities (EEG), eye movement (EOG), muscle activities (EMG), heart rhythm (ECG), respiratory flow, respiratory efforts and pulse oximetery.

The EEG (electroencephalogram) monitors brain waves and can be used to determine the level of sleep or wakefulness.

The EOG (electro-oculogram) measures eye movements using sticker electrodes placed next to each eye. This measurement can help determine the duration of REM sleep.

An EMG (electromyogram) measures muscle movements. It may include measuring both chin and leg movement or one of them. It helps to determine the duration of REM sleep.

The respiratory flow is measured with a nasal/oral cannula fitted near the nostrils and connected to pressure transducer. This allows measuring breathing rate and also monitoring the breathing cessation.

Respiratory efforts are measured by the use of two belts. Belts are fastened around the chest and abdomen of patient to record the chest and abdomen wall movements respectively. The belts typically use piezoelectric sensors or respiratory inductance plethysmography (RIP) techniques.

Pulse oximetry is used to monitor the changes in the blood oxygen level during sleep. Pulse oximetry can detect the oxygen saturation which allows a way for detection apnea and hypopnea events.

Below is an example of summary report of polysomnoghraghy (Kushida, Littner, & Morgenthaler, 2005).

> Mr. J., age 41, 5'8" tall, 265 lbs., came to the sleep lab to rule out obstructive sleep apnea. He complains of some snoring and daytime sleepiness. His score on the Epworth Sleepiness Scale is elevated at 15 (out of possible 24 points), affirming excessive daytime sleepiness (normal is <10/24).
>
> This single-night diagnostic sleep study shows evidence for obstructive sleep apnea (OSA). For the full night his apnea+hypopnea index was elevated at 18.1 events/hr. (normal <5 events/hr; this is "moderate" OSA). While sleeping supine, his AHI was twice that, at 37.1 events/hr. He also had some oxygen desaturation; for 11% of sleep time his SaO2 was between 80% and 90%.
>
> Results of this study indicate Mr. J. would benefit from CPAP. To this end, I recommend that he return to the lab for a CPAP titration study.

To detect sleep apnea disorders, recording *respiratory flow*, *respiratory efforts* and *changes in oxygen level* is mandatory in PSG. The indicators for recording these signals have been added to the PSG after identifying sleep disorder sleep apnea in 1970s. Figure 13(a) shows the patient monitored for sleep breathing disorder in a sleep lab and Figure 13(b) depicts a typical view of ploysomnography.

(a)

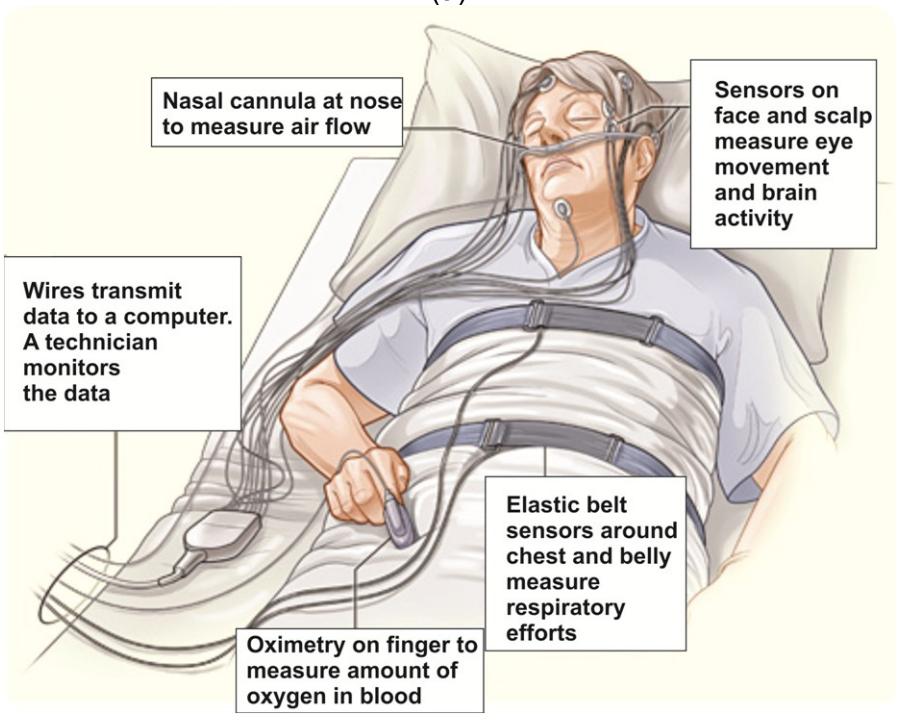

(b)

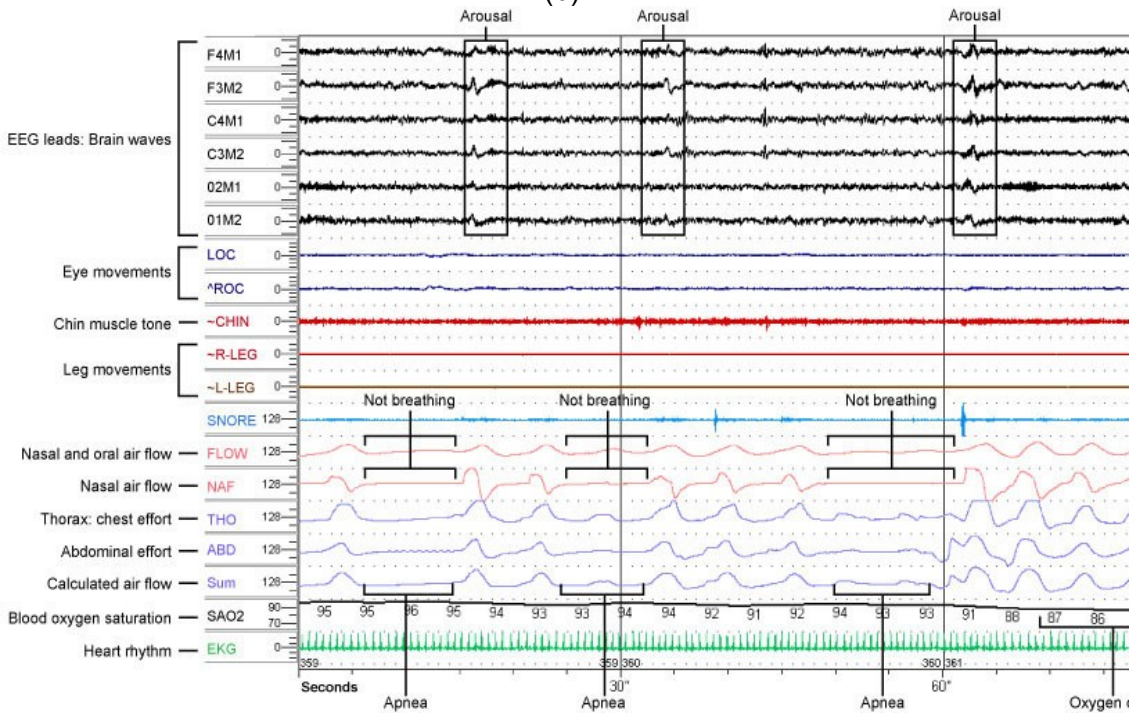

Figure 13. ***(a) a patient monitored for sleep breathing disorder.(b) a typical view of polysomnography (My test sleep, 2012)***

Advantages of PSG

Advantages of PSG include the following:

- Since the PSG is performed at special sleep centers with attending sleep technicians, technicians are continuously present to adjust signals for optimal recording.
- Sleep and its different stages are recorded
- Several sleep disorders or conditions may be observed.

Disadvantages of PSG

Disadvantages of PSG include:

- PSG is expensive and time consuming for the patient and evaluator
- The complex set-up required for sleep testing may affect sleep architecture, resulting in inaccurate results.
- Misplacement of the equipment may result in inconclusive results or inaccurate readings
- PSG is an overnight test performed at special sleep centers which needs the patients spend at least one night in an unfamiliar environment.
- Due to the paucity of sleep centers and the long waiting list, patients who are referred to sleep centers need to wait for a long time from 4 weeks to 6 months to be scheduled for PSG.

2.4.2. *Home Sleep Test*

As mentioned in previous section, polysomnography (PSG) is the gold standard for the diagnosis of sleep apnea. However, for some patients, home sleep tests (HSTs) can be used to diagnose this condition. PSG and HSTs use the same respiratory equipment, pulse oximetry equipment, and movement and position sensors (Ballester, Solans, Vila X, Hernandez, Quintó, & Bolivar, 2000).

Figure 14 shows the *Embletta gold device* and the way that is worn by a person.

(a) (b)

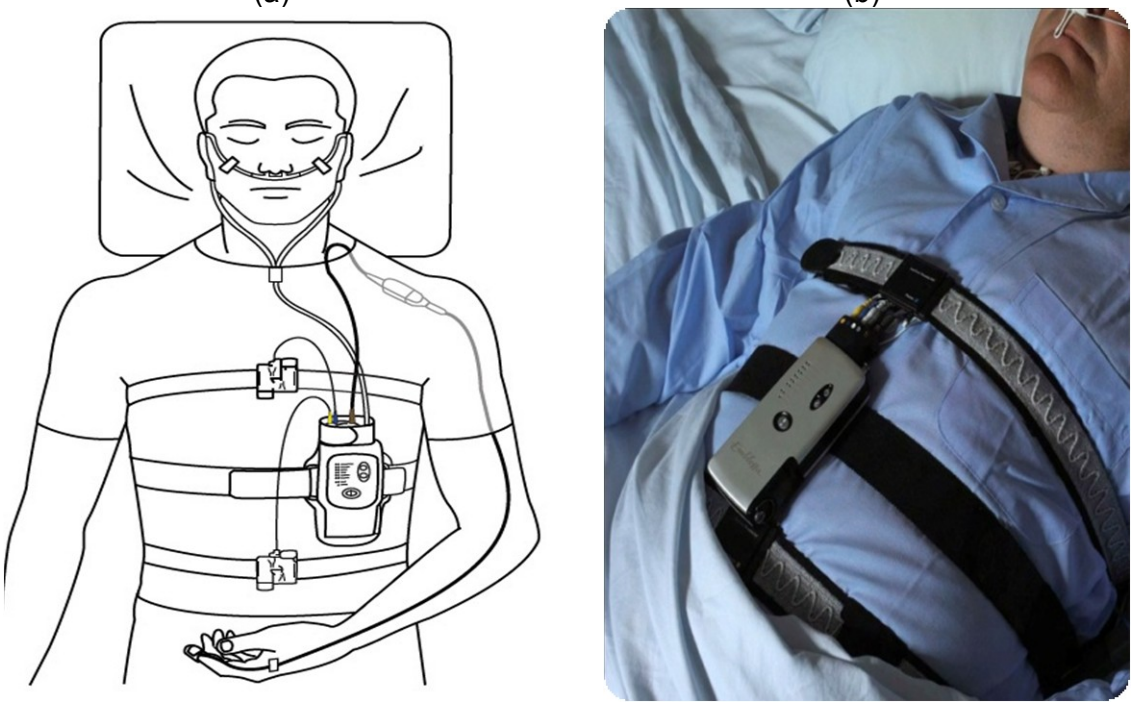

Figure 14. Home sleep test (a) Typical set-up for home sleep test. (b) image of patient with HST in place. Images of Embletta gold device (Embla systems, 2010).

Embletta gold device is a standard home testing device by Embla® (Embela systems, 2011). Embletta gold device can record the following channels (Embla systems, 2010):

- Flow pressure (nasal cannula)
- Oral pressure (thermistor)
- XFlow* (with XactTrace RIP belts)
- Snore (Nasal Pressure)
- Differential pressure
- Abdominal movement (with XactTrace RIP belts)
- Thoracic movement (with XactTrace RIP belts)
- Sp02 average (oximeter)
- Sp02 beat to beat (oximeter)
- Pulse rate (oximeter)

- Pulse waveform (oximeter)
- Body position Activity
- Event marker
- EKG
- EEG
- EOG

This device can be sold to the patients by or under an order of a physician.

Multiple studies have been done to demonstrate the sensitivity and accuracy of HSTs (Whittle, Finch, Mortimore, MacKay, & Douglas, 1997) ,(PORTIER & PORTMANN, 2000). Machines that have been studied include Edentec, PolyG, AutoSet, Embletta, Sibel Home, Bedbugg, NovaSom, WatchPAT, SNAP, ApneaLink, SOMNOcheck, Stardust II, Apnomonitor, and Apnea Risk Evaluation System (ARES) Unicorder. Although these studies only validated the individual machine that was tested, the aggregate results of these studies indicated that HSTs, in general, provide an accurate and reproducible method of identifying patients with OSA.

Advantages of HSTs

Advantages of HSTs include the following (Collop, et al., 2007):

- Recording is performed in a familiar environment.
- HSTs are substantially less expensive and more widely available than in-facility PSGs.
- No known risks are associated with home sleep tests (HSTs).

Disadvantages of HSTs

Disadvantages of HSTs include (Collop, et al., 2007):

- The limited capability to immediately identify and resolve technical issues
- The inability to diagnose other types of sleep disorders,
- An increased role for the patient in terms of the application and use of the device, which may make some patients uncomfortable.
- The total sleep time cannot be calculated from an HST recording, since sleep and wake states are not directly assessed.

- As with PSG, improperly preparing the patient for HST or misplacement of the equipment may result in inconclusive results or inaccurate readings; however, with an HST, no attendant is present to solve these issues as they arise, so the patient may have to repeat the study.

Types of HST Monitors

Three categories of portable monitors (Type II, III, and IV) are used in the diagnosis of OSA in either an attended or unattended setting.

2.5. New approaches to sleep apnea diagnosis

The overnight full channel polysomnography involves comprehensive recording of biophysiological changes during sleep. The whole process is complex, cumbersome to patients and costly. Simplified testing at home is possible for selected patients (Chesson, Berry, & Pack, 2003) but uses the same basic respiratory measurement techniques as described above. The complex set-up required for sleep testing may affect sleep architecture, resulting in inaccurate results. Therefore, there is a considerable interest in development of reliable and simple low cost techniques for the identification of individuals with sleep breathing disorders.

Since the sleep apnea is classified as a breathing disorder and also due to difficulties in measuring respiratory activity, indirect measurement of respiratory airflow and efforts has drawn much attention in recent years. Several investigators have attempted to monitor the indirect quantities of airflow in upper airway or extract the respiratory efforts. Following sections briefly discuss the studies that have been proposed for this purpose.

2.5.1. *Sleep apnea monitoring based on ECG Derived Respiration (EDR)*

Derivation of respiratory signals from Multi-lead ECGs was suggested by Moody et al. (Moody G. B., Mark, Zocco, & Mantero, 1985) in *Computers in Cardiology* 1985 for the first time. In this study Moody et al. showed that the expansion and contraction of the

chest due to respiration results in motion of chest electrodes and changes the electrical impedance of the thoracic cavity. These physical influences of respiration result in amplitude variations in the observed ECG which can be extracted by mean of signal processing methods as the respiratory waveform called ECG Derived Respiratory(EDR).

Detecting sleep apnea was suggested by Moody et al. as one of the applications of the ECG Derived Respiration (EDR) (Moody G. B., et al., 1986).

The respiratory waveform extracted from ordinary Electrocardiogram (ECG), as Moody et al. suggested, was considered as the respiratory efforts and was used for identifying Cheyne-Stokes respiration and central sleep apnea with confidence but not for monitoring obstructive sleep apnea (Moody, et al., 1986).

Since Moody et al released the idea of using EDR in monitoring sleep apnea, many investigators have attempted to study the different signal processing methods for extracting respiratory waveform from ECG (de Chazal, Heneghan, Sheridan, Reilly, Nolan, & O'Malley, 2003)and expand its applications in identifying both obstructive and central sleep apnea (Mendez, et al., 2010) and (Gubbi & Khandoker, 2012) , (de Chazal, Heneghan, Sheridan, Reilly, Nolan, & O'Malley, 2003) and (Decker, et al., 2010)

Although extracting the respiratory patterns would be useful and convenient in many situations in which the ECG, but not respiration, is routinely monitored, however the extracted respiratory signal is generated by the electrode motion relative to the heart and by the changes in the thoracic electrical impedance as lungs fill and empty. Thus, these methods are limited to the manifestation of respiratory effort and do not provide information about the upper airway flow. For cases of obstructive sleep apnea when the respiratory efforts is present but there is no air entering the airways or lungs such methodologies fail to properly detect the apnea periods.

2.5.2. *Sleep apnea monitoring base on thoracic impedance derived respiratory*

In the recent years, several studies have been conducted to extract the respiratory waveform from thoracic impedance and also assess the validation of thoracic

impedance derived respiratory (Ernst, Litvack, Lozano, Cacioppo, & Berntson, 1999), (Houtveen, Groot, & de Geus, 2006), (Seppa, Viik, & Hyttinen, 2010).

In the recent research conducted by Seppa et al. (Seppa, Viik, & Hyttinen, 2010), for the first time, the suitability of impedance pneumography (IP) for measurement of continuous pulmonary flow and volume signals was assessed.

Since the changes in the thoracic impedance are influenced by the movement of chest which accompanies the respiration, the thoracic impedance derived respiratory waveform reflects the respiratory efforts. Therefore, the estimated flow obtained by calculating the differentiation of thoracic impedance derived respiratory, as suggested by Seppa et al. (Seppa, Viik, & Hyttinen, 2010), cannot reflect the real quantities of airflow in the upper airway. Thus, just like the EDR, thoracic impedance respiratory signals are not reliable for detecting obstruction in upper airway in case of sleep apnea.

2.5.3. *Sleep apnea monitoring and diagnosis based on tracheal respiratory sounds*

As an alternative method, different features of tracheal and lung sound have been used to estimate the respiratory flow (Yadollahi & Mousavi, 2006), (Que, Kolmaga, Durand, Kelly, & Macklem, 2002), (Yap & Moussavi, 2002). In addition, the application of acoustical respiratory flow in detecting sleep apnea was investigated in several studies (Yadollahi & Moussavi 2010).

Although there are some robust methods for estimating the respiratory flow from tracheal sounds (Yadollahi & Mousavi, 2006), these methods are efficient for detection of deep breathing only. In case of low breath (below 0.3 liters/s), when the sound amplitude does not exceed the background noise, detecting the relationship between the sound amplitude and the air flow is very difficult (Que, Kolmaga, Durand, Kelly, & Macklem, 2002). More importantly, these methods are limited to the estimation of flow and are not useful at monitoring the respiratory efforts which reduces their applications in full sleep apnea analysis as registered in PSG.

2.5.4. *Sleep apnea monitoring base on accelerometer*

Development of MEMS accelerometers has induced a new wave of approaches to estimate respiratory signals based on the measurement of upper-body acceleration (Morillo, Ojeda, Foix, & Jim, 2010), (Bates, Ling, Mann, & Arvind, 2010), (Reinvuo, Hannula, Sorvoja, & Alasaa, 2006) and (Phan, Bonnet, Guillemaud, & Castelli, 2008).

In a recent investigation performed by Morillo et al. (Morillo, Ojeda, Foix, & Jim, 2010), the respiratory flow waveform has been extracted from an accelerometer mounted on the suprasternal notch of subjects resting supine. Although the method proposed in this study estimated the *respiration rate* with a low error there was no result presenting the correlation between the estimated flow signal and the reference respiratory signal. In addition, the estimated flow was limited to the supine position, which hampers the generality of the findings. Furthermore, this method does not provide means of measuring the respiratory efforts which are essential in sleep apnea monitoring. It is worth noting that in this study, the heart rhythm and snoring pitches were also extracted from acceleration signal which would be clinically useful and convenient.

Methods proposed by Reinvuo et al. (Reinvuo, Hannula, Sorvoja, & Alasaa, 2006), Bates et al. (Bates, Ling, Mann, & Arvind, 2010) and Phan et al. (Phan, Bonnet, Guillemaud, & Castelli, 2008) used accelerometers for the same purposes but again, they are all limited to the estimation of *respiration rate* and their ability to derive continuous flow or volume waveform signals was neither investigated nor claimed.

In our previous study conducted by Dehkordi et al. (Dehkordi, Marzencki, Tavakolian, Kaminska, & Kaminska, 2011), the same author of this thesis, inspired by the extensive studies carried on seismocardiogram (Tavakolian, Vaseghi, & Kaminska, 2008)and also the research by Morillo et al (Morillo, Ojeda, Foix, & Jim, 2010), we demonstrated the preliminary results proving that the use of a small tri-axial MEMS accelerometer mounted on the suprasternal notch allows for indirect evaluation of respiratory flow in different sleep postures (supine, prone and lateral) and different flow rates (tidal, deep and shallow).

With respect to the waveform morphology, the result of this study (Dehkordi, Marzencki, Tavakolian, Kaminska, & Kaminska, 2011) demonstrated that the

Accelerometer Derived Respiratory (ADR) signal is strongly correlated to the reference spirometry signal.

Figure 15 shows 30 second segments of accelerometer derived respiratory and recorded spirometry signal in the side position and three different flow rates.

The mean value of the correlation coefficient between ADR and reference spirometry signal for all subjects and conditions estimated as 0.88 (σ= 0.09). Figure 16 presents the cross patient mean correlation coefficient values and standard deviations for different positions and breath patterns for ADR and spirometry.

The relative error of breathing rates calculated by using the accelerometer signal and the spirometry signal was very low (1.5%) in three different postures (supine, lateral and prone) across all subjects. Table 1 summarizes the mean values of the absolute value of the relative error of breathing rates obtained from the ADR and the breath rates obtained from the spirometry signals in the three different postures across all subjects.

The study conclusions were that employing an accelerometer, placed on the suprasternal notch could potentially provide an estimation of the flow waveform. In the current study, we have expanded our work to measure the respiratory efforts as well as the respiratory flow.

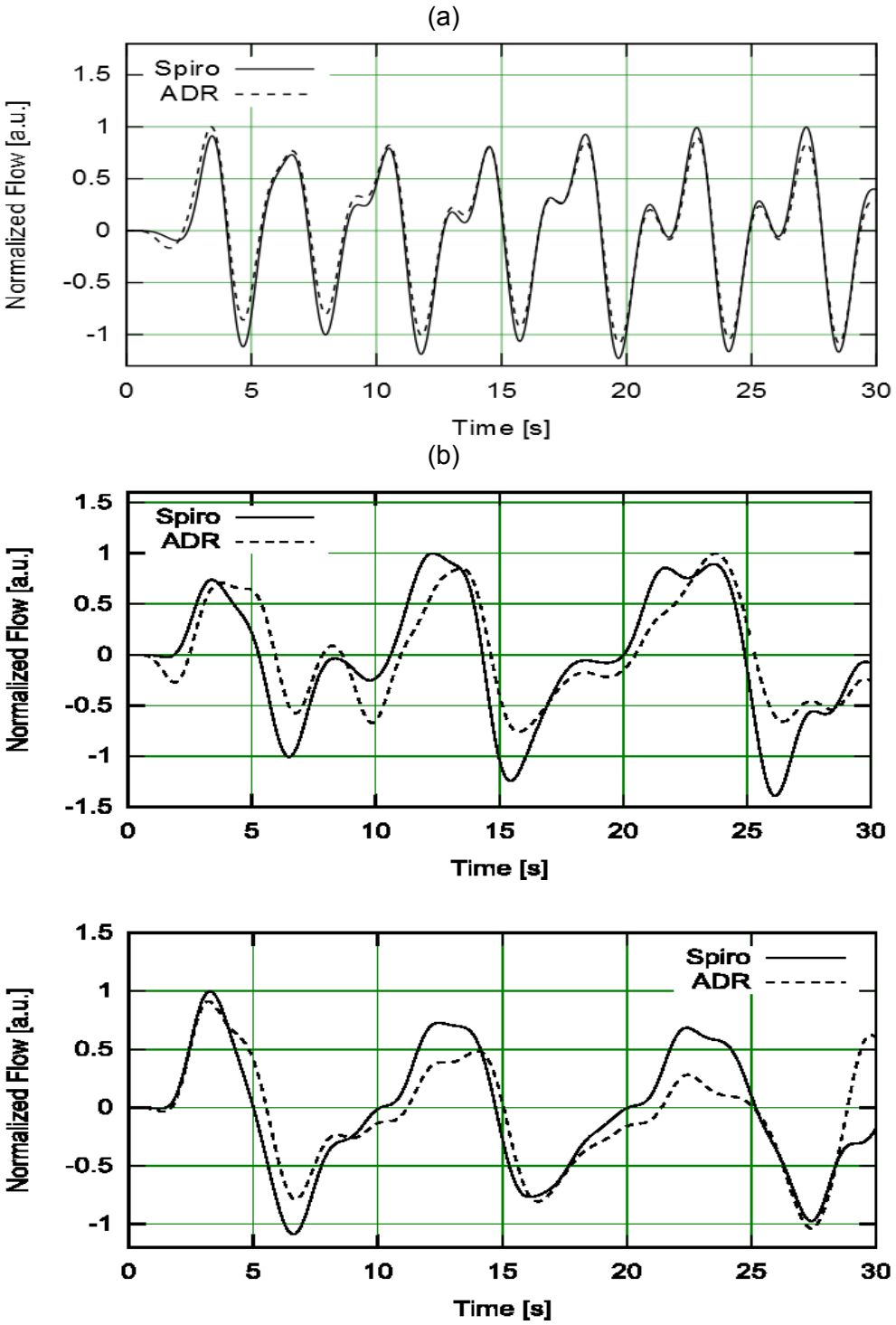

Figure 15. ***Examples of normalized flow rates for the three breath patterns used it this study acquired with standard spirometry (Spiro) and ADR (acceleration derived respiratory)***

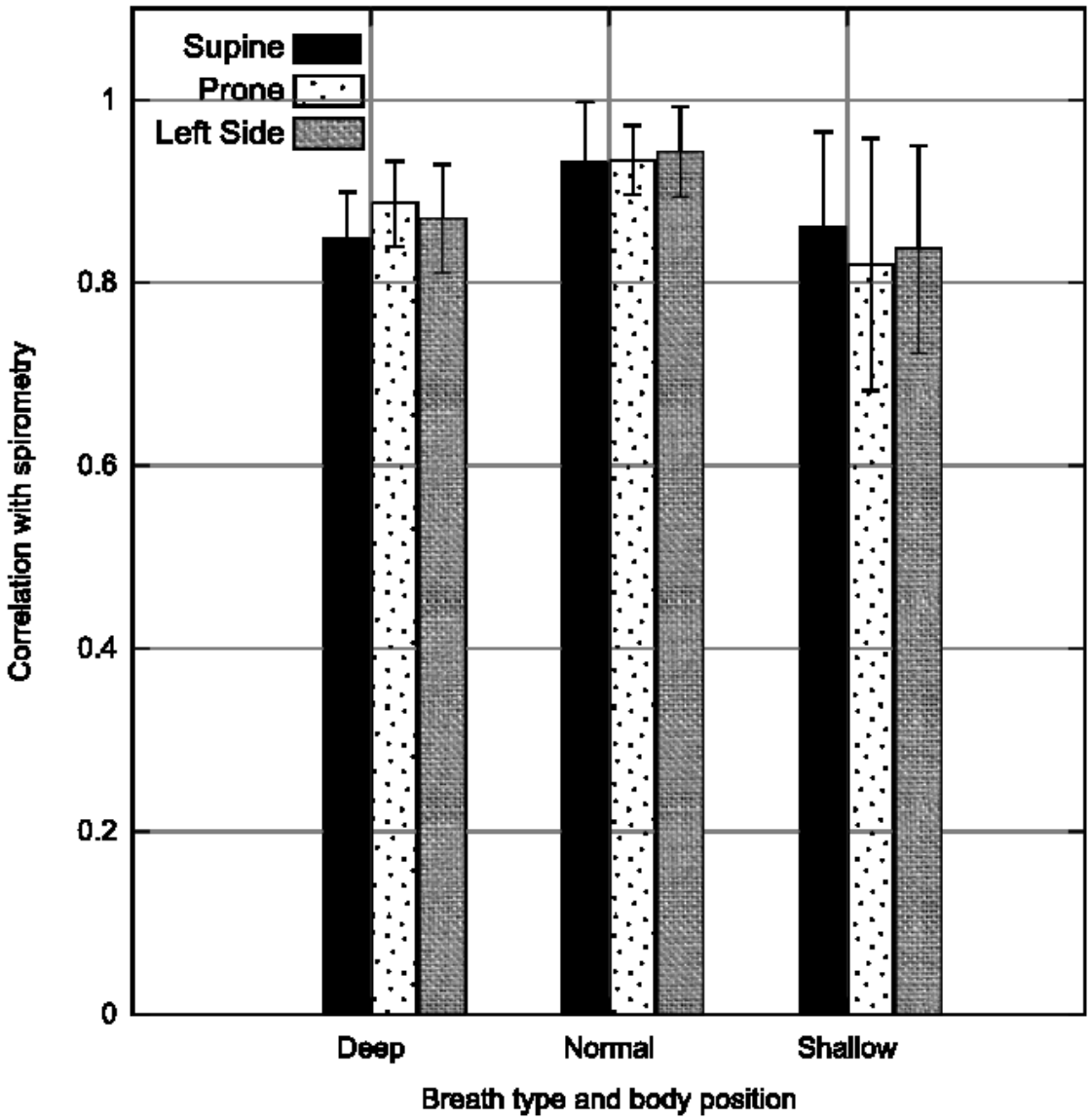

Figure 16. Correlation between acceleration derived respiratory signal and spirometry in three different positions (supine, prone and left side) and different flow rates(deep, normal and shallow breathing)

Table 1. The absolute relative error of breathing rates obtained for ADR (acceleration derived respiratory) relative to spirometry

	Supine	Prone	Left side	Overall
ADR	1.61%	1.63%	1.40%	1.55%

2.6. Machine Learning Techniques

Machine learning is a set of techniques for design and development of algorithms to induce patterns or rules from past experiences. The past experiences are presented by the collected datasets. A learner (a computer program) processes the collected data of past experiences to describe the data in the meaningful way or find the appropriate response to future experiences. In the other word, machine learning focuses on the prediction, based on known properties learned from the training data.

There are three major categories of learning:

1) Supervised in which the machine is provided the expected output and trained to respond correctly.
2) Unsupervised in which the machine is provided with no knowledge beforehand of expected output and trained to discover structures in presented inputs
3) Reinforcement in which the machine is not provided with explicit output instead it is periodically given performance indicators.

Since in this study the supervised learning was used to induce the desired results, this method is described briefly in the next section.

2.6.1. *Supervised learning*

Supervised learning is the machine learning task of inferring a function from *supervised* training data. The following notations are used in the rest of this thesis for supervised learning:

- $x^{(i)}$: input variable or input feature
- $y^{(i)}$: output or target variable.
- $(x^{(i)}, y^{(i)})$: a training example
- X: Space of input variables.
- Y: Space of output variables
- Training set: a list of m training examples $\{(x^{(i)}, y^{(i)}); i = 1, \ldots, m\}$. It is the dataset which is used for learning.

In the supervised learning problem, the goal is to learn a function f: X → Y so that $f^{(x)}$ is a “good” predictor for the corresponding value of y. The supervised learning process is showed in Figure 17.

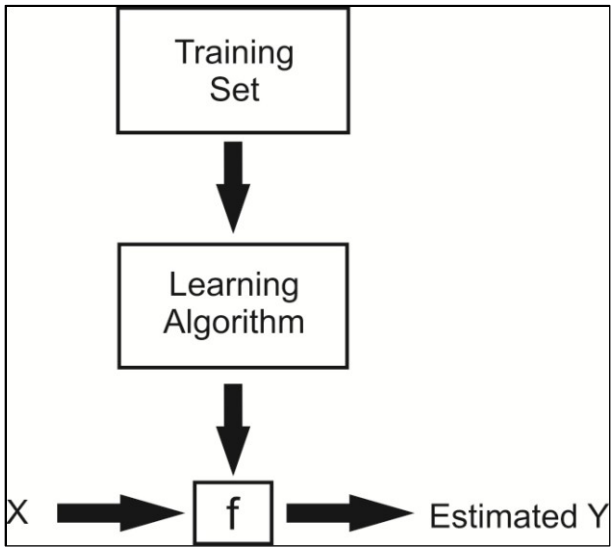

Figure 17. Schematic supervised learning

When the output variable that we’re trying to predict is continuous, the learning problem is called a *regression* problem. When y can take on only a small number of discrete values, we call it a *classification* problem. There are a large number of methods available for fitting models to continuous variables, such as a linear regression, nonlinear regression, regression trees, Neural Networks and etc. (Hastie, Tibshirani, & Friedman, 2009).

In order to assess accuracy of a predictor, we need to define a *loss function* $L(y, f(\mathbf{x}))$, where y is true output, and $f(\mathbf{x})$ is the predictor. Loss function is sometimes denoted with R (risk function).

2.6.2. *Time Domain Impulse Response Using Correlation Analysis (IR)*

Time-domain correlation analysis refers to nonparametric estimation of the impulse response of dynamic systems from the data as a finite impulse response (FIR) model. In correlation analysis a linear system is assumed which does not require a specific model structure (Keesman, 2011).

Impulse response is the output signal that results when the input is an impulse and has the following definition for a discrete model:

$$u(t) = 0, t > 0$$
$$u(t) = 1, t = 0$$

The response to an input u(t) is equal to the convolution of the impulse response, as follows:

$$y(t) = \int_0^t h(t-z).u(z)dz$$

To better understand the algorithm of *correlation analysis*, consider the following description of a dynamic system:

$$y(t) = G(q)u(t) + v(t)$$

where u(t) and y(t) are the input and output signals, respectively. v(t) is the additive noise term. G(q) is the transfer function of the system. The G(q)u(t) notation represents the following operation:

$$G(q)u(t) = \sum_{k=1}^{\infty} g(k)u(t-k)$$

q is the shift *operator*, defined by the following equation:

$$G(q) = \sum_{k=1}^{\infty} g(k)q^{-k}$$

$$q^{-1}u(t) = u(t-1)$$

For impulse response, the algorithm estimates impulse response coefficients *g* for both the single- and multiple-output data. The impulse response is estimated as a high-order, noncausal FIR model:

$$y(t) = g(-m)u(t+m) + \ldots + g(-1)u(t+1)$$
$$+ g(0)u(t) + g(1)u(t-1) + \ldots + g(n)u(t-n)$$

The estimation algorithm prefilters the data such that the input is as white as possible. It then computes the correlations from the prefiltered data to obtain the FIR coefficients.

The system identification toolbox of Matlab (Mathworks, 2011) was used for the implementation of this method in this study.

2.6.3. *Artificial Neural Network (ANN)*

Artificial neural networks have been extremely valuable for learning from examples (Nayak, Jain, & Ting, 2001). ANNs have been successfully applied to a wide range of pattern recognition and function approximation problems and generated interest from researchers in such different areas as engineering, medicine, computer science, psychology, neuroscience, physics, and mathematics.

ANNs represent the computational structure that is based on the way biological nervous systems, such as the brain, process information.

An ANN consists of one or more layers of nodes configured in regular and highly connected topologies. The nodes are interconnected via unidirectional signal channels called links. The commonest type of ANN consists of three layers: an input layer (consists of input nodes), an output layer (consists of output nodes) and a hidden layer (consists of hidden nodes). Raw information is fed into the network via input nodes. The activities of input nodes along with the weights on links between input and hidden nodes determine outputs of hidden nodes. Behaviour of the output nodes depends on the activities of hidden nodes and the weights on links between hidden and output nodes.

A feed forward network allows signals to move from input to output nodes only. There is no feedback from output to input/hidden nodes or lateral connections among the same layer. A feedback network allows signals to travel in both directions by introducing loops in the network.

There are single-layer and multi-layer architectures. In single layer architectures, for example the Hopfield model (Sammut & Webb, Encyclopedia of Machine Learning, 2010), a single layer of nodes forms the topology. The output from each node feed back to all of its neighbours; whereas in multi layer architectures, several layers of nodes form the topology.

Neural networks have capability of transforming inputs into desired output changes; this is called neural network learning or training. These changes are generally produced by sequentially applying input values to the network while adjusting network weights.

A feed forward neural network trained by back propagation was implemented for this method. Few different structures were tried and finally, a structure with two hidden layers (ten neurons in the first layer and five neurons in the second layer) and one neuron in the output layer was selected. Each neural network was trained and tested five times, and the output was calculated by averaging the five output results. The neural network toolbox of Matlab (Mathworks, 2011) was used.

2.6.4. *MARSpline*

MARSplines is a nonparametric regression procedure that makes no assumption about relationship between the input and output variables of a model. Instead, MARSplines is a procedure for fitting adaptive non-linear regression that uses piece-wise linear basis functions to define relationships between an output variable and a set of predictors (or input variables) (Hastie, Tibshirani, & Friedman, 2009). The resulting regression surface is piecewise linear and continuous.

2.6.5. *Ensemble learning*

Ensemble learning is a procedure of training multiple learning machines and combining their outputs to achieve a 'committee' of decision makers. The principle is that the decision of the committee should have better overall accuracy, on average, than any individual committee member (Sammut & Webb, 2010). Several studies have demonstrated that ensemble models very often achieve higher accuracy than single models (Sammut & Webb, 2010). The members of the ensemble might be predicting real-valued numbers, class labels, posterior probabilities, rankings, clusterings, or any other quantity. Therefore, their decisions can be combined by many methods, including averaging, voting, and probabilistic methods.

Motivation

If we could build the "perfect" machine learning device, one which would give us the best possible answer every time, there would be no need for ensemble learning methods. Ensemble learning comes from this recognition that in real-world situations, every model has limitations and will make errors. Considering this reality that each model has these "limitations," the aim of ensemble learning is to manage their strengths and weaknesses, leading to the best possible decision being taken overall.

Methods and Algorithms

An ensemble consists of a set of models and a method to combine them. This section begins by assuming that there exists a set of models, generated by any of the learning algorithms; we describe several popular methods of combining their outputs for regression problems.

Methods for Combining a Set of Models

There are several methods for model combination. The linear combiner and the product combiner are the most common methods used so far in different applications.

The linear combiner is used for models that output real-valued numbers, so is applicable for regression ensembles. The notation for linear combiner is defined in equation (1) where $f(x)_i$ for $i = 1..n$ is a machine learning model and n shows the number of models.

$$CE = \sum_{i=1}^{n} w_i f(x)_i \qquad 2\text{-}1)$$

If the weights $w_i = 1/n$, $\forall i$, this turns to a simple averaging of models.

Another common combiner is the product rule defined in equation (2) where Z is a normalization factor.

$$CE = \frac{1}{z} \prod_{i=1}^{n} f(x)_i \qquad 2\text{-}2)$$

We have discussed only two combiner rules. Numerous other rules exist, including methods for combining rankings of classes, and unsupervised methods to combine clustering results.

3. The proposed sleep apnea analysis

3.1. Introduction

The objective of this study is to estimate the respiratory flow and efforts using signals recorded by three tri-axial MEMS accelerometers placed on the upper-body of subjects.

Inspired by the extensive studies carried on seismocardiogram (Tavakolian, Vaseghi, & Kaminska, 2008) which showed the possibility of extracting the respiratory effort from the acceleration of chest and also the research by Morillo et al. (Morillo, Ojeda, Foix, & Jim, 2010) which presented the feasibility of extracting flow waveform from the acceleration of suprasternal notch, we employed an approach for detecting sleep apnea base on upper body acceleration.

In this study three accelerometers were placed on:

1) The suprasternal notch to indirectly quantify the airflow in the upper airway,
2) The left seventh intercostal space to monitor the chest wall movement and,
3) The abdomen to monitor the abdominal movement.

The respiratory flow signal was estimated from the acceleration of suprasternal notch, the rib cage and abdomen recorded by three accelerometers.

The thoracic respiratory effort was estimated from the signal recorded by the accelerometer mounted on the left seventh intercostal space of subjects' rib cage.

The abdominal respiratory effort was estimated from the signal obtained by the accelerometer placed on the abdomen wall.

The machine learning and ensemble learning techniques were adapted for estimating desired signals.

This method allows for indirect detection of airflow cessation events in order to detect apnea periods, and detection of respiratory efforts in order to classify the apnea events into obstructive and central. To assess the agreement between estimated signals and the reference signals recorded by well-established measurement methods, we compared the estimated flow to the oronasal flow signal picked up by a nasal/oral cannula and compared the estimated respiratory efforts to the readings obtained with two strain gauge belts.

This chapter discuss data acquisition process , the signal processing steps employed for indirect monitoring of respiratory flow and efforts and the validation procedure.

3.2. Data acquisition

3.2.1. *Participants*

The participants for this study were volunteers from Simon Fraser University with no history of cardiopulmonary disorders. The measurement procedure, setup and the purpose of study were described in detail to them. The subjects were not rewarded nor given any benefit. The experiment was performed under the ethics approval from Simon Fraser University.

The test population consisted of 20 participants, 17 male and 3 female. Except for one participant, who was 60 years old, the subjects were between 24 and 35 years old. None were suffering from obesity and none were smokers.

3.2.2. *Test Setup*

The dataset of this study was collected at Center for Interactive Bio-Engineering Research (CiBER) laboratory, applied science faculty, Simon Fraser University.

The data acquisition involved measurement of:

- Three-lead ECG
- Nasal/oral airflow (F_{nasal})
- Thorax respiratory effort (V_{Th})
- Abdominal respiratory effort (V_{Abd}),
- Acceleration (three axis of measurement) of the suprasternal notch (ACC_S), the thorax (ACC_{Th}) and the abdomen (ACC_{Abd}).

The nasal/oral airflow was obtained with a nasal & oral cannula (Model 0589, Braebon Canada, Kanata, ON) connected to a pressure sensor (Model 0585, Braebon Canada, Kanata, ON). The pressure sensor was calibrated using a water manometer.

The respiratory efforts were recorded using two respiratory effort transducers (Model SS5LB, BioPac Systems Inc, Camino Goleta, CA) mounted on two elastic belts. The belts were fastened around the thorax and abdomen to measure the changes in thoracic and abdominal circumference respectively.

The acceleration signals were acquired with three ADXL335z tri-axis MEMS accelerometers (Analog Devices Inc, Norwood, MA). The accelerometers were placed on the suprasternal notch, the thorax and the abdomen using a double-sided polyurethane foam tape (3M, Maplewood, MN) and further secured using an over-the-top single sided paper tape.

Data acquisition was performed with a data acquisition system NI9205 (National Instruments, Austin, TX). All signals were digitized at the rate of 500 Hz.

Finally, data storage was performed on a personal computer running a custom built LabVIEW Virtual Instrument (VI).

The schematic diagram of data acquisition system is illustrated in Figure 18. This figure shows the placement of sensors and their connection to acquisition system.

Figure 19 shows the data acquisition setup for simultaneous recording of ECG, the nasal/oral flow, the respiratory efforts and upper body acceleration.

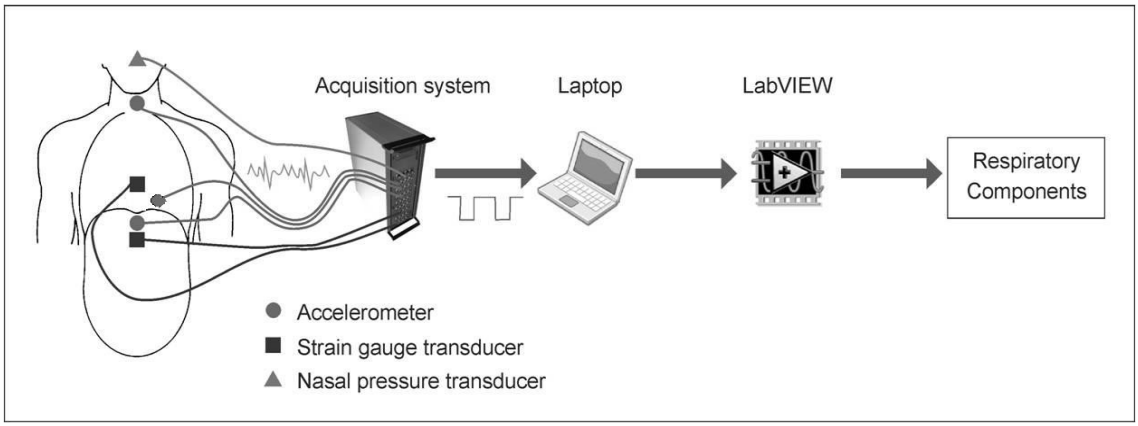

Figure 18. Schematic diagram of data acquisition system

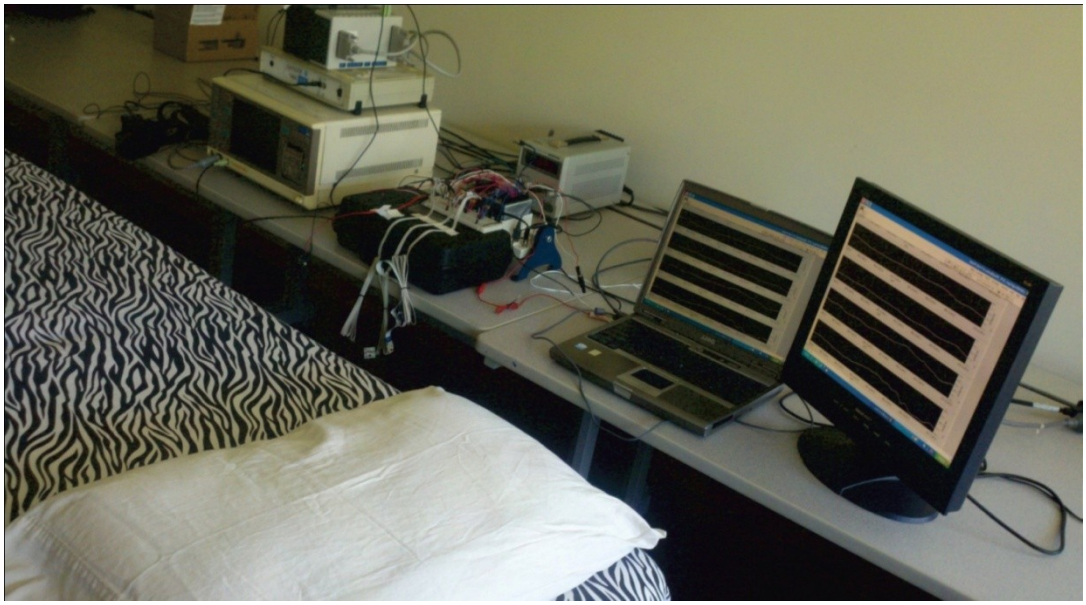

Figure 19. Complete acquisition setup for simultaneous acquisition of ECG, the oral/nasal flow, the respiratory efforts and acceleration of upper body.

Figure 20 shows a subject lying on side during data acquisition and also emplacement of three accelerometers, two belts and a nasal cannula.

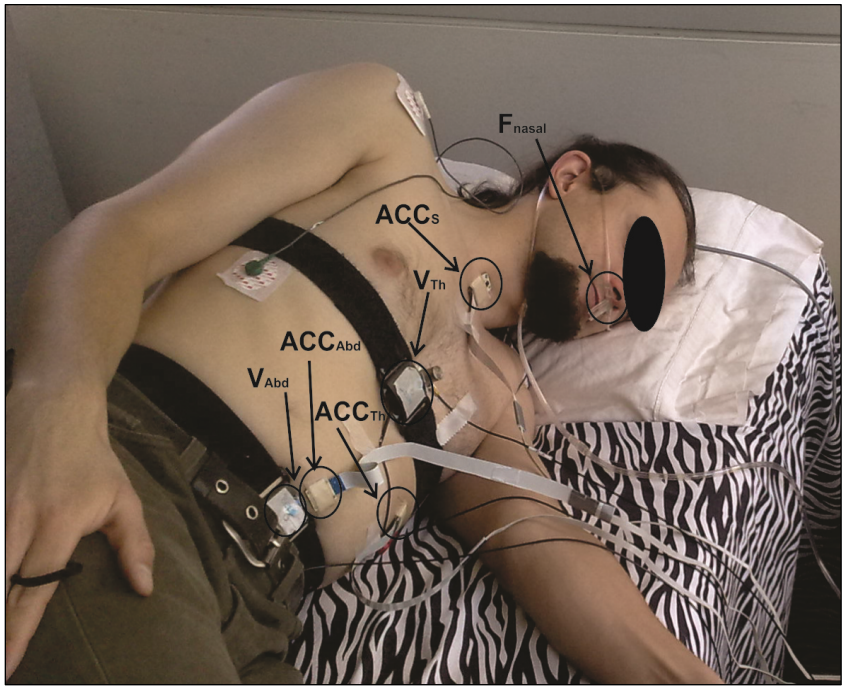

Figure 20. The complete measurement equipment setup in CiER Lab with focus on emplacement of three accelerometers, two belts and a nasal cannula. Photo is shown with the permission of subject.

Figure 21 depicts an accelerometer mounted on suprasternal notch of a subject. The subject was wearing a nasal/oral cannula too.

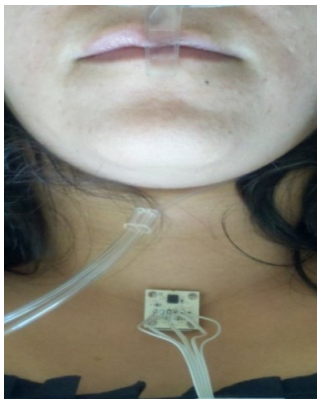

Figure 21. Emplacement of an accelerometer on suprasternal notch of a subject in CiBER lab. Subject is wearing nasal cannula too.

3.2.3. *Position of three accelerometers*

As shown in Figure 22, for this study, the three accelerometers were mounted on suprasternal notch, the right seventh rib interspace and abdomen below the subjects' umbilicus.

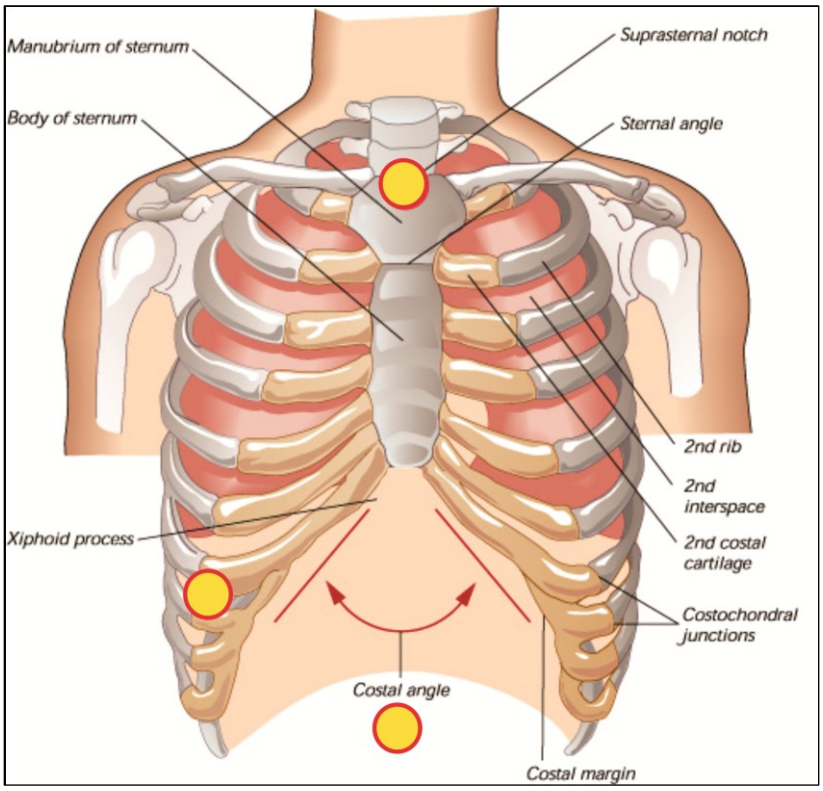

Figure 22. Position of three accelerometers on torso

Inspired by the study of Morrilo et al. (Morillo, Ojeda, Foix, & Jim, 2010), for measuring the acceleration of the upper airway due to respiratory flow, we selected suprasternal notch for placement of one of the three accelerometers.

For measuring the thorax respiratory effort, we used the signals recorded by another accelerometer placed on the subjects' right seventh rib interspace. To find the best location on the thorax for placing the accelerometer, two options were examined. Considering the results presented by Morillo et al. (Morillo, Ojeda, Foix, & Jim, 2010) and

by Tavakolian et al. (Tavakolian, Vaseghi, & Kaminska, 2008), we recorded the thorax acceleration from accelerometers mounted on Xiphoid and the right seventh rib interspace simultaneously. After analyzing the signals, the right seventh rib interspace was chosen that minimized the overall estimation error.

The third accelerometer was placed on the subjects' abdomen below the umbilicus to record the movement of abdomen wall due to respiratory activity.

3.2.4. *Procedure*

The experimental session for each subject lasted for 35 minutes on average.

Subjects were briefly introduced to a control breathing pattern before signal recording. According to the control breathing pattern, the subjects were ask to breathe at 2 different flow rates (tidal and deep) with about 5 breaths at each rate followed by a 12 seconds of breath hold after the deep breathing period.

For each subject, we recorded two sets of control breathing signals. The two recording sets lasted 2 and 3 minutes respectively and constituted the training and test datasets for the signal processing phase.

The measurement procedure was carried out while subjects were in supine, prone and lateral positions. A brief pause was introduced between each change of conditions to allow the subject to rest and relax.

Due to technical problems, parts of signals of 3 subjects were discarded.

3.3. Data analyse and processing

Figure 23 shows the major steps of data analysis and processing employed in this study: (1) pre-processing, (2) signal estimation and (3) statistical analysis. These steps were entirely performed using MATLAB as described below.

Noise removal, normalization and signal segmentation were performed in *pre-processing phase*.

The purpose of *signal estimation phase* was to identify and customize models to estimate the flow signal and the thorax and abdominal respiratory effort signals.

In *statistical analysis step*, the validity of estimated signals was assessed in several different ways.

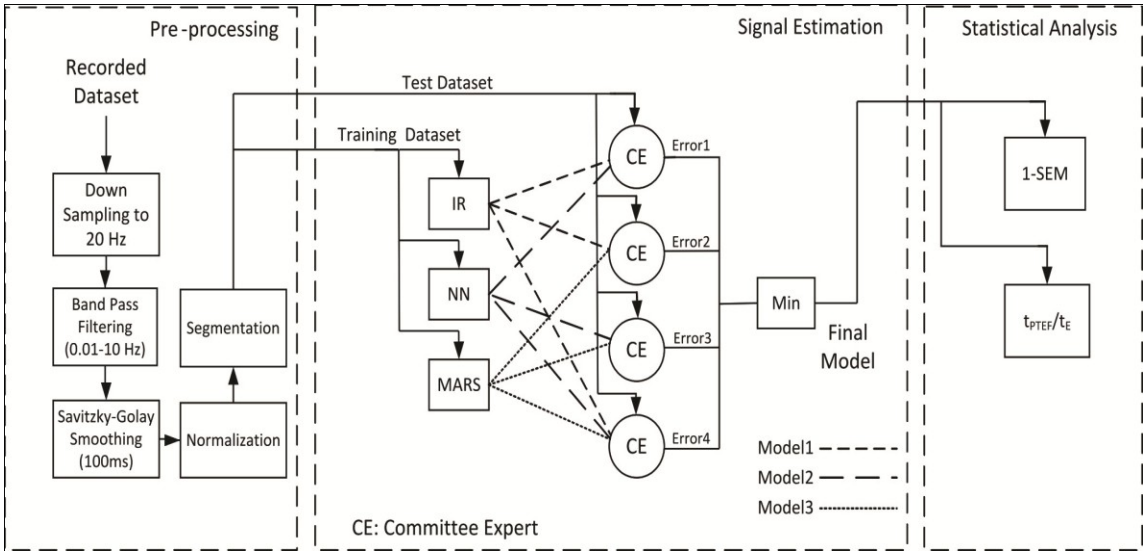

Figure 23. Schematic representation of data analysis and signal processing including pre-processing, signal estimation and statistical analysis. In signal estimation step the committee with IR and NN models as the members (grey circle) was chosen as the final model due to its role in producing the minimum error.

3.3.1. *Preprocessing*

Figure 24 shows the acceleration of suprasternal notch in three directions recorded by the three-axial memes accelerometer. All the signals depicted in these figures are raw signals before being pre-processed.

The purpose of the pre-processing step was to remove instrumentation noise, baseline fluctuations and cardiac related contents. Signal segmentation was performed in this step too.

The following shows the pre-processing steps. First, all signals recorded from the three accelerometers (ACC_S, ACC_{Th}, and ACC_{Abd}), the nasal cannula (F_{nasal}) and the thorax and abdomen belts (V_{Th} and V_{Abd}) were down sampled to 20 Hz.

To remove the instrumentation noise and baseline fluctuations, as recommended by Bates et al. (Bates, Schmalisch, & Stocks, 2000), all signals were treated with the band pass filters, in the range of 0.1 and 10 Hz.

For removing the seismocardiogram contents from the signals, a Savitzky-Golay smoothing filter, and frame size 100 ms, second order fitting, was used (Savitzky & Golay, 1964). This filter has the advantage of preserving the high frequency contents of the signal while effectively removing the cardiac related contents.

The glitches were annotated manually and removed from signals .Then all signals were normalized.

Finally, to analyze the breathing signals at different flow rates, the signals were segmented into tidal and deep segments using F_{nasal} as the trigger. The segmentation was done manually.

The effect of prepossessing phase was illustrated in figures from 24 to 27. Figure 24 illustrates the recorded nasal flow, thorax and abdomen belt signals and Figure 25 shows the acceleration of suprasternal notch in three directions before pre-processing step. The signals depicted in Figure 24 and Figure 25 were recorded simultaneously from one subject.

The Figure 26 and Figure 27 show the same signals of Figure 24 and Figure 25 respectively after preprocessing.

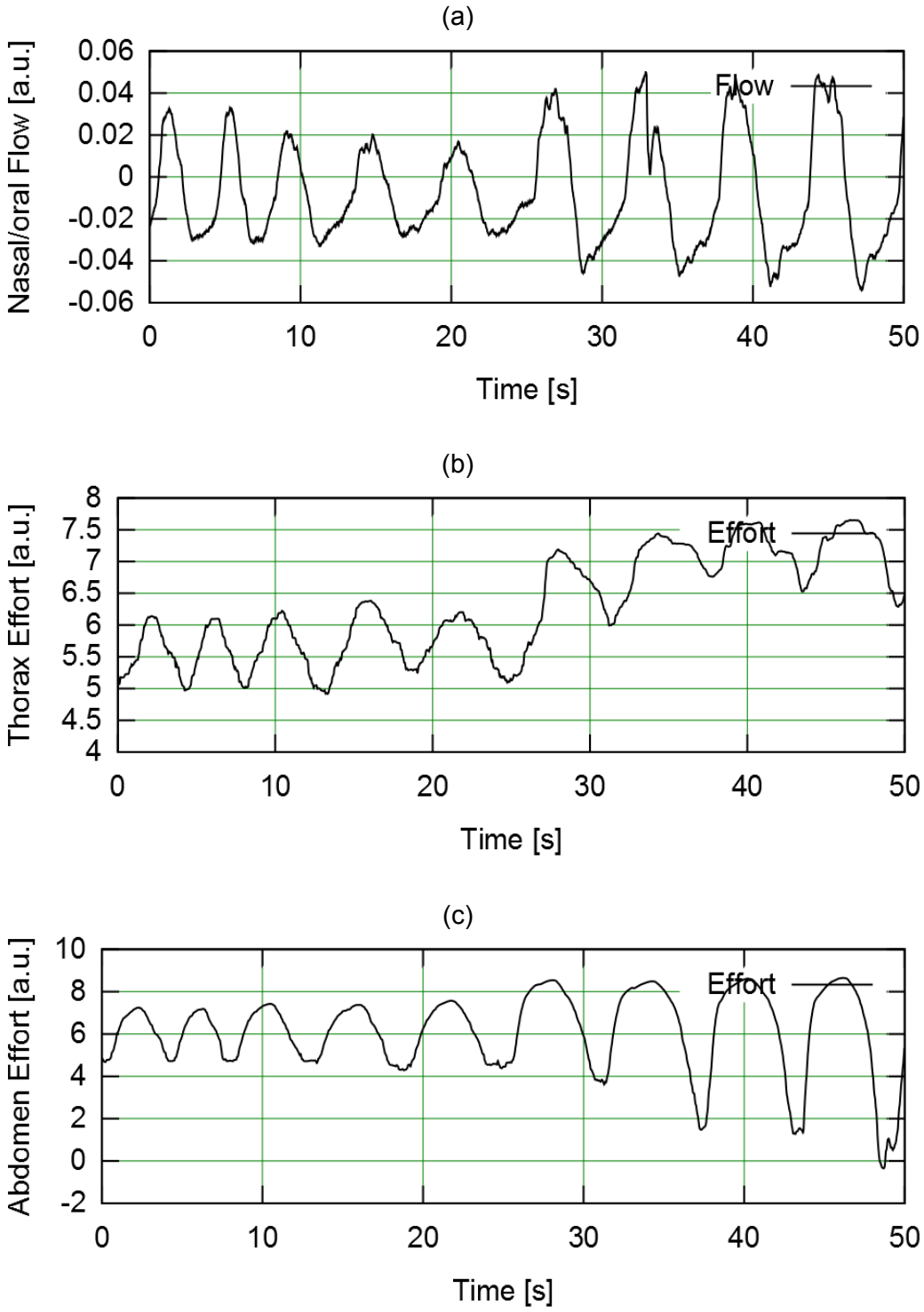

Figure 24. ***The 50-second segments of (a) Nasal/oral flow, (b) thorax respiratory effort and (c) abdominal respiratory effort before preprocessing.***

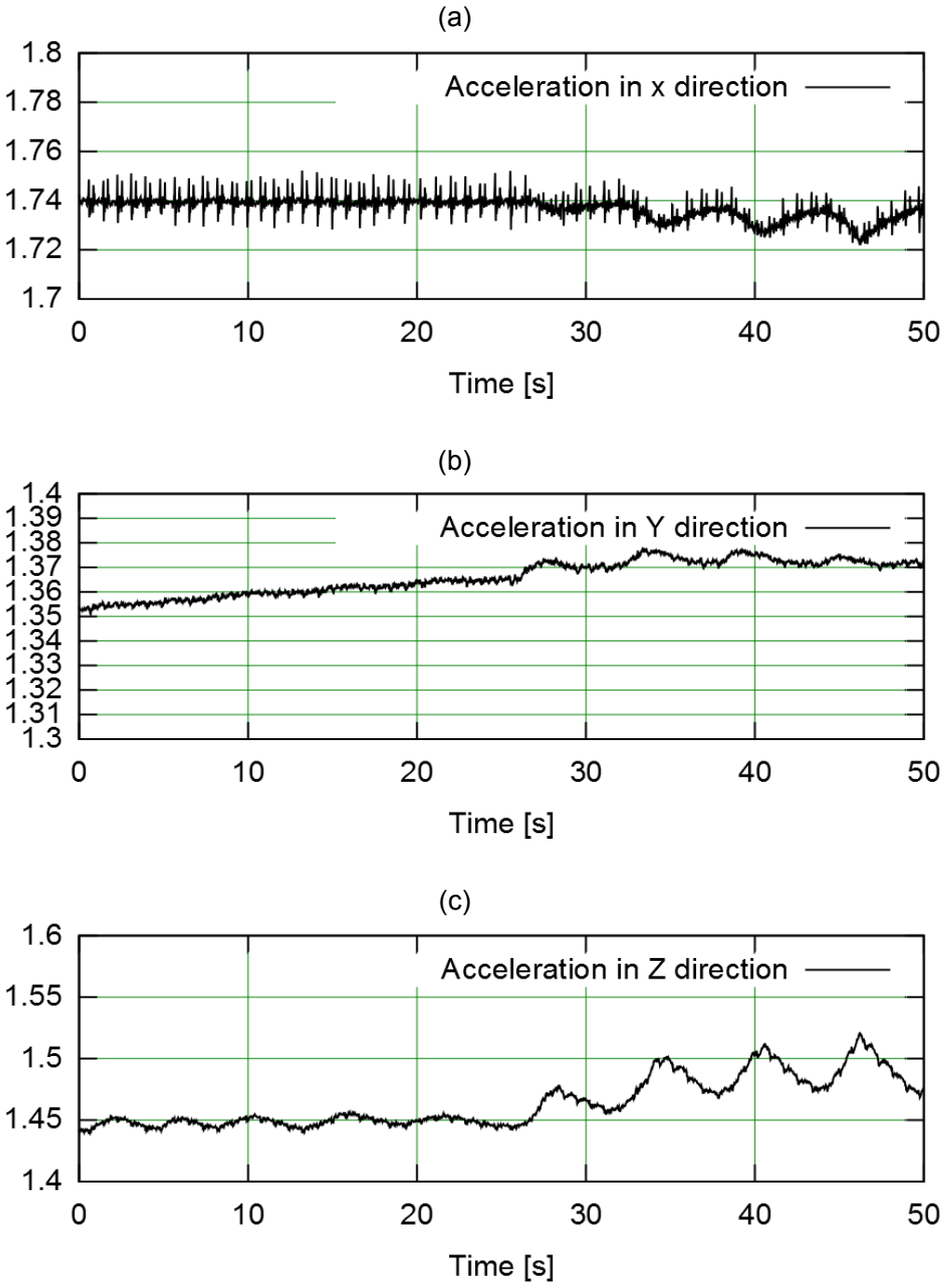

Figure 25. ***The acceleration of suprasternal notch in (a) x direction, (b) y direction and (c) z direction recorded by a three-axial mems accelerometer. The depicted signals are raw signals before pre-processing.***

Note. The signals recorded simultaneously with the signals of Figure 23 from the same subject.

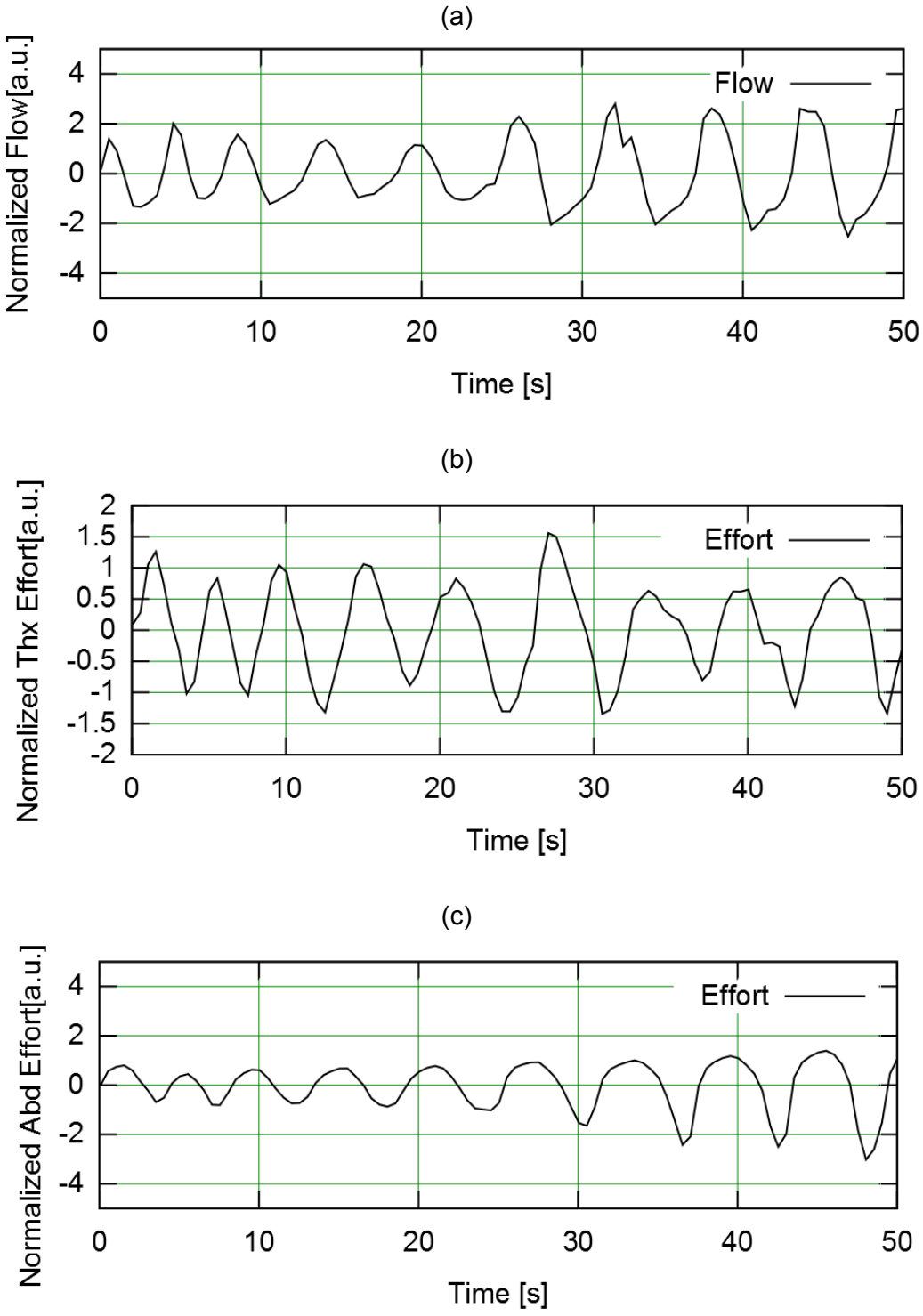

Figure 26. ***The same 50-second segments of (a) Nasal/oral flow, (b) thorax respiratory effort and (c) abdominal respiratory effort as the Figure 23 after preprocessing.***

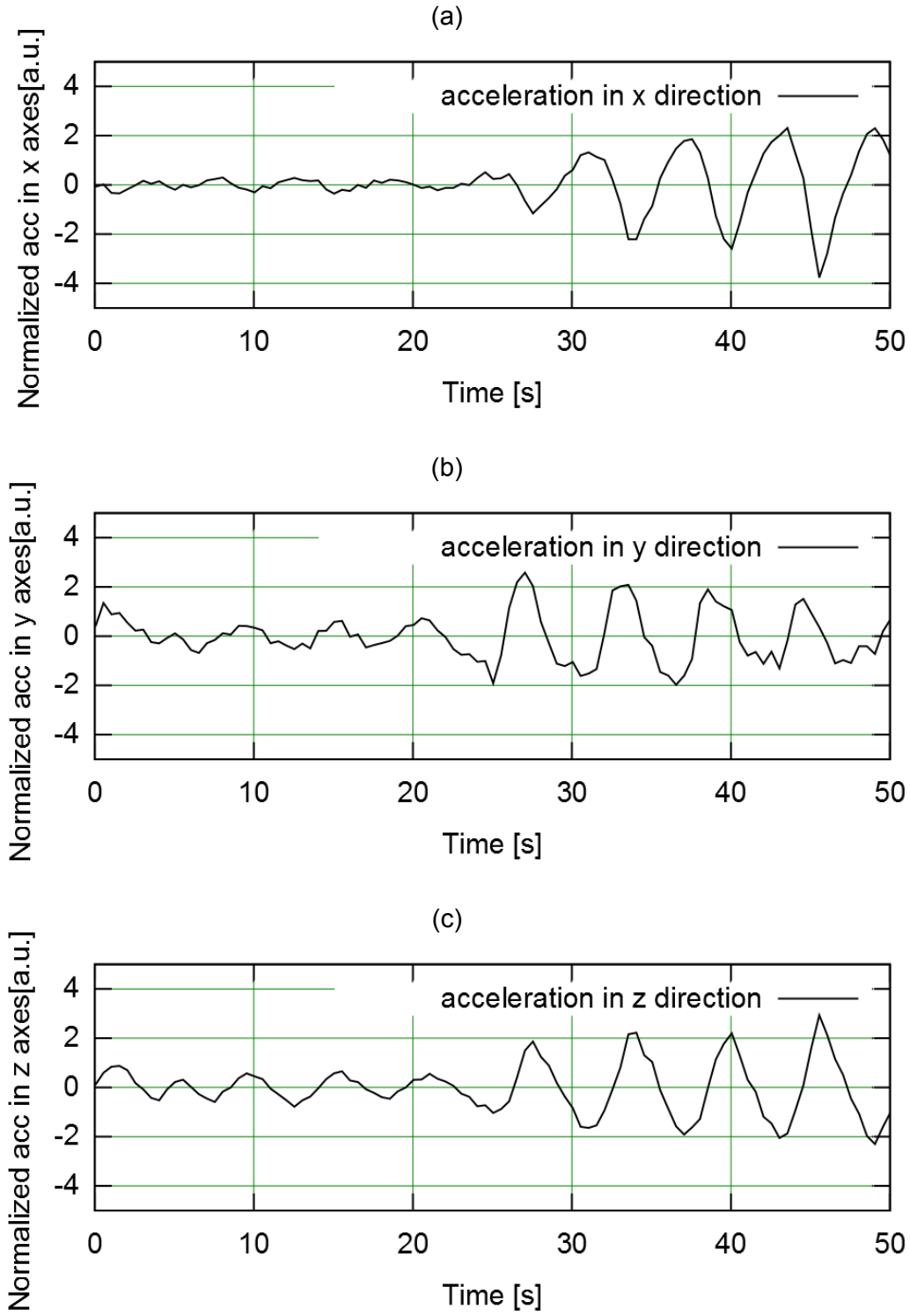

Figure 27. ***The acceleration of suprasternal notch in (a) x direction, (b) y direction and (c) z direction recorded by a three-axial mems accelerometer. The depicted signals are as the same signal of Figure 24 after pre-processing steps.***

3.3.2. *Signal Estimation*

Signal estimation block of Figure 23 illustrated the overall view of a patient-specific approach used for signal estimation in this study. In this method the separate training and test procedures were performed for every individual subject. It means that for each subject different models were customized by using the data of training set in different postures (supine, lateral and prone) and flow rates (tidal and high) and after that the desired signals, respiratory flow and efforts were estimated by feeding the test data to the customized models.

Respiratory Flow Estimation (F_{est})

Three models were trained(model1, model2 and model3 in Figure 23) by feeding the training set of each subject to IR, NN and MARS methods and customizing them separately for each subject. Suprasternal notch acceleration (ACC_S), thorax wall acceleration (ACC_{Th}), and abdomen wall acceleration (ACC_{Abd}) were considered as the input variables and F_{nasal} was used as the output variable (Figure 23).

After customizing the three models with three different machine learning methods, an ensemble learning approach was employed to combine the outputs of models, treating them as a committee of experts. The principle of ensemble learning is that the decision of the committee should have better overall accuracy, on average, than any individual committee member (Sammut & Webb, Encyclopedia of Machine Learning, 2010). As shown in Figure 23 , the outputs of three models combined in four different ways to build four different committees: three committees including two by two combinations of these models and one committee including all three of them as member. The combination of three models is as following:

- Model1(FIR) and model2(NN)
- Model1(FIR) and model3(MARS)
- Model2(NN) and model3(MARS)
- Model1(FIR) and model2(NN) and model3(MARS)

The models were combined using the very simple average linear combiner (Sammut & Webb, Encyclopedia of Machine Learning, 2010) as defined in Eq. 2-1**)** .

The outputs of committees were applied to the test dataset to estimate respiratory flow F_{est}.

The flowchart illustrated in Figure 28 briefly presents taken steps for estimating respiratory flow from ACC_S, ACC_{Th}, and ACC_{Abd}. In this flowchart the combination of model1 (FIR) and model2 (NN) as the members of one of the committees is shown.

We repeated this process for the recorded data in all conditions and different flow rates. The committee which minimized the overall Standard Error Measurement (SEM), described in section 3.3.3, for the estimated flow in compare with reference flow was chosen as the final committee. The committee with the FIR and NN models as the members was investigated as the final committee at the end of signal estimation step.

Thorax Respiratory Effort Estimation

The same approach for the flow estimation was employed for the thorax respiratory effort estimation. However, for customizing the models, the thorax acceleration (ACC_{Th}) was used as the input variable and the thorax belt signal V_{Th} was taken as the output variable. The models were combined by the same average combiner in Eq. 2-1**)** to result four committees. The committee which minimized the overall Standard Error Measurement (SEM) for the estimated thorax effort in compare with the reference thorax belt signal was chosen as the final committee. The committee with the non-causal FIR and neural network models as the members was investigated as the final committee to estimate the final thorax respiratory effort.

Abdominal Respiratory Effort Estimation

This section follows the thorax respiratory effort estimation: we trained the models using the abdominal acceleration ACC_{Abd} as the input variable and the abdomen belt signal V_{Abd} as the output variable. The models were combined by the same average combiner in Eq. 2-1**)** to result four committees. The committee which minimized the overall Standard Error Measurement (SEM) for the estimated abdominal effort in compare with the reference abdomen belt signal was chosen as the final committee. The committee with the non-causal FIR and neural network models as the members was investigated as the final committee to estimate the final abdominal respiratory effort.

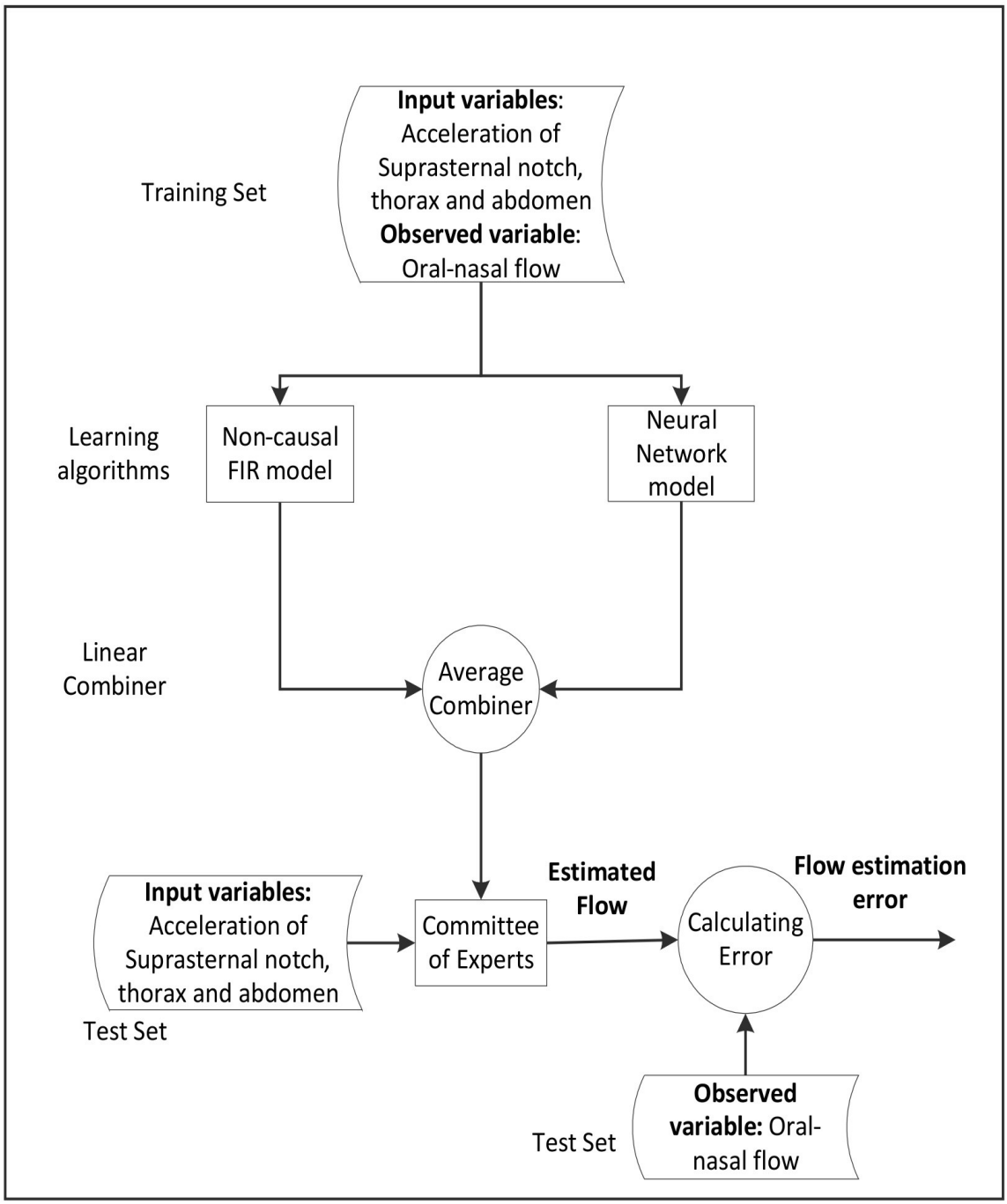

Figure 28. ***The flowchart of taken steps to estimate respiratory flow from acceleration of suprasternal notch, thorax and abdomen. Non-causal FIR model and neural network model were trained by applying training set of each subject in every condition. The customized models were combined by an average combiner to result a committee of experts.***

3.3.3. *Statistical Analysis*

In order to assess the agreement between the estimated respiratory flow (F_{est}) and the actual measured value (F_{nasal}), a Standard Error Measurement (SEM) value as defined in equation 3-1 was used, where *n* is the size of each segment.

$$\rho = 1 - SEM = 1 - \frac{\frac{1}{n}\sum_{i=1}^{n}\left[F_{nasal}(i) - F_{est}(i)\right]^2}{Var(F_{nasal})} \qquad 3\text{-}1)$$

The value of ρ reflects the similarity of the F_{nasal} and F_{est} signals calculated sample by sample. Value ρ = 1 means that the signals are identical, a value below 1 means that the signals are different in some degree (Seppa, Viik, & Hyttinen, 2010).

Agreement between the estimated thorax respiratory effort (E_{Th}) and the thorax belt signal (V_{Th}) was evaluated in the same way as defined in equation ***3-2***).

$$\rho = 1 - SEM = 1 - \frac{\frac{1}{n}\sum_{i=1}^{n}\left[V_{Th}(i) - E_{Th}(i)\right]^2}{Var(V_{Th})} \qquad 3\text{-}2)$$

The abdominal respiratory effort agreement, ρ, for estimated abdomen respiratory effort (E_{Abd}) and the abdomen belt signal (V_{Abd}) was assessed in the same was as defined in equation 3-3).

$$\rho = 1 - SEM = 1 - \frac{\frac{1}{n}\sum_{i=1}^{n}\left[V_{Abd}(i) - E_{Abd}(i)\right]^2}{Var(V_{Abd})} \qquad 3\text{-}3)$$

4. Results

4.1. Introduction

In this chapter the performance of proposed method for monitoring sleep apnea using the upper body acceleration presented in chapter 3 was examined.

As mentioned in section 3.3.2, the system identification approach was conducted for estimating desired signals in this study. To fulfil the requirements of this approach, the recorded experimental data base of this study was divided into the two separate sets: the training data set for identifying the models and the test date set for estimating the signals in interest and also making the decision about the validity of identified models.

For each subject, lying down in three different postures and breathing in three different rates, the upper airway flow and the thoracic and the abdominal respiratory efforts were estimated as defined before. Then the statistical analysis presented in 3.3.3 was performed to validate the estimated signals in respect to the reference signals which were recorded with well-established measurement methods. This chapter presents the results of the assessment of the validity of estimated signals.

4.2. Validation of estimated flow

Time domain finite impulse response, neural network and MARS methods were used for estimating the flow signal from the acceleration of suprasternal notch, the rib cage and abdomen. The committee of experts with the time domain finite impulse response and the neural network models as members minimized the estimation error in respect to the reference nasal/oral flow (F_{nasal}) and was chosen as the final model to estimate the flow signal (F_{est}).

A typical example of the reference flow signal (F_{nasal}) recorded by nasal cannula and the estimated flow signal (F_{est}) in Figure 29 shows that the estimated signal follows the reference flow perfectly in tidal and deep cycles and also in cessation periods.

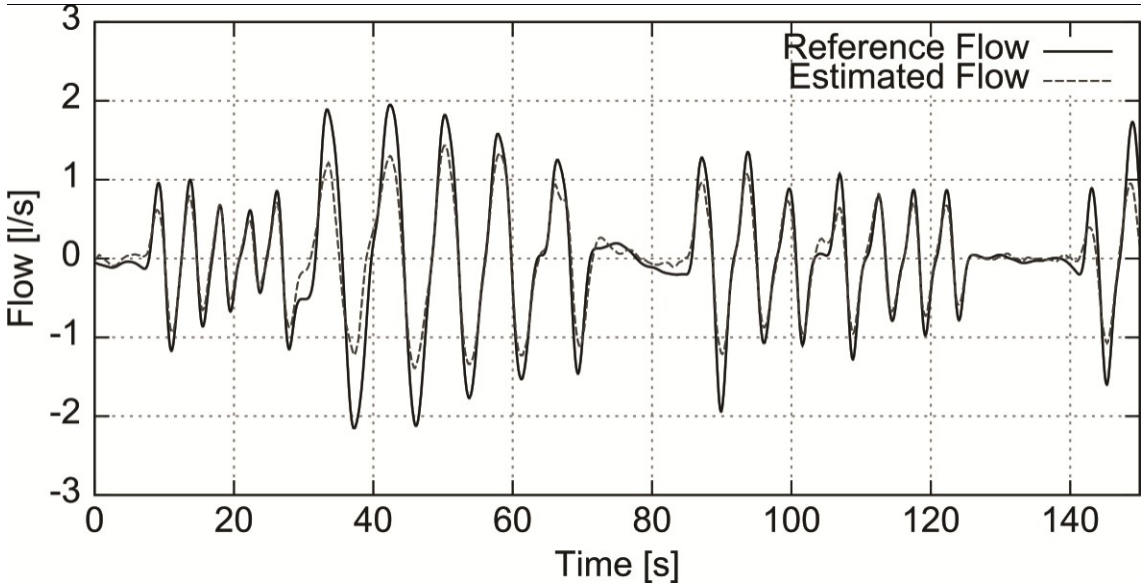

Figure 29. An example of the actual (solid line) and estimated flow (dashed line). The estimated flow follows the reference signal in tidal and deep breathing and also in apnea periods.

The validity of the estimated flow in respect to the recorded nasal/oral signal was examined in four different ways as follow:

1. Calculating ρ for the estimated respiratory flow and the recorded nasal/oral flow using the equation 3-1.
2. Comparing the start time of breathing cessations in the estimated flow signal and the recorded nasal/oral flow signal.
3. Comparing the values of t_{PTIF}/t_I calculated for each cycle of the estimated flow signal and recorded nasal/oral flow signal.
4. Comparing the values of t_{PTEF}/t_E calculated for each cycle of the estimated signal and recorded nasal/oral flow signal.

4.2.1. *Flow agreement*

For each subject, the ρ values calculated for F_{est} and F_{nasal} in different positions and flow rates are presented in Table 2. In this table “M” and “F” denote the mate and female subjects respectively. Label “-“ denotes a completely unsuccessful recording.

The entries of this table were summarized as (mean-standard deviation) for men and women in two different diagrams in Figure 30.

Table 2. ***Individual agreement between the estimated (F_{est}) and reference flow (F_{nasal})***

S	Gender	Supine			Prone			Lateral		
		Tidal	Deep	Mix	Tidal	Deep	Mix	Tidal	Deep	Mix
1	M	0.8753	0.8573	0.8468	0.7653	0.904	0.8736	0.88	0.6728	0.675
2	M	0.9317	0.7921	0.8183	0.9277	0.8687	0.8864	0.8387	0.6828	0.695
3	M	0.8602	0.9723	0.8917	0.88	0.7283	0.6429	0.9305	0.8717	0.8761
4	M	0.848	0.8863	0.8641	0.8403	0.8881	0.8673	0.9233	0.8167	0.8477
5	M	0.8856	0.7662	0.7501	0.858	0.8778	0.8741	0.7698	0.7668	0.534
6	M	0.9007	0.8278	0.8321	0.8234	0.6049	0.6203	0.6401	0.8406	0.8343
7	M	0.7745	0.6995	0.678	0.6521	0.776	0.7703	0.7024	0.7573	0.7711
8	M	0.9129	0.9348	0.9245	0.8564	0.8421	0.8196	0.9183	0.8299	0.8174
9	M	0.944	0.8861	0.8884	0.7554	0.8944	0.8721	0.6755	0.8098	0.7946
10	F	0.759	0.7557	0.7326	0.862	0.8259	0.7911	0.8511	-	-
11	M	0.7607	0.8669	0.8678	0.8425	0.8729	0.8029	0.7734	0.8701	0.8426
12	F	0.879	0.9197	0.8944	0.81	0.72	0.67	0.766	0.7309	0.7126
13	M	0.8772	0.8722	0.8632	0.7762	0.8333	0.8049	0.8062	0.8299	0.8252
14	M	0.6646	0.8996	0.893	0.782	0.7951	0.791	0.8651	0.892	0.8909
15	M	0.7494	0.9456	0.9148	0.6233	0.9223	0.8926	0.8774	0.9141	0.8998
16	M	0.7696	0.9527	0.8543	0.7813	0.7306	0.7021	0.9375	0.8398	0.8257
17	M	0.79	0.8362	0.8221	0.81	0.7945	-	0.7276	0.9429	0.9063
18	F	-	0.8658	0.8623	-	0.7013	0.687	0.92	0.8683	0.8431
19	M	0.7047	0.8175	0.8071	0.7389	0.8423	0.808	0.8732	0.8344	0.8206
20	M	0.7747	0.9461	0.9327	-	-	-	0.904	0.918	0.9151

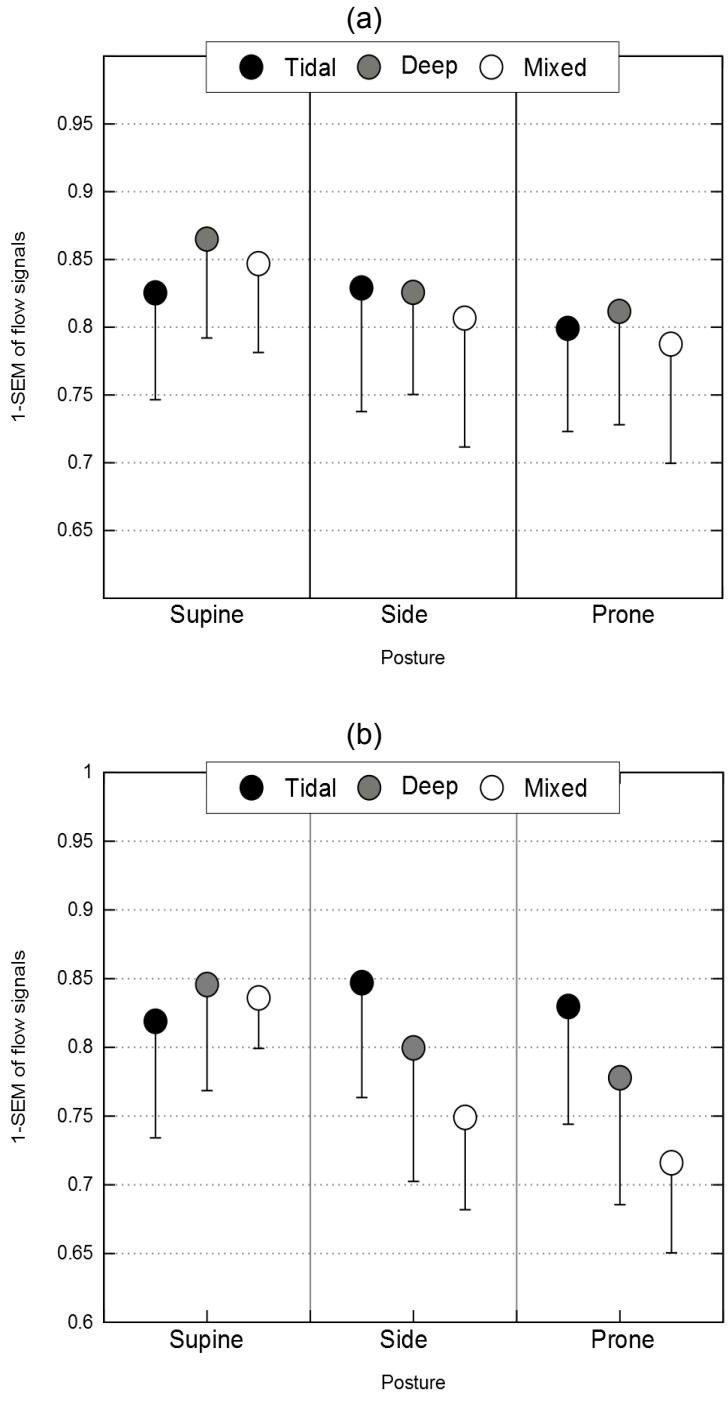

Figure 30. ***Waveform agreement (1-SEM) between Fest and Fnasal expressed as mean-SD for (a) male subjects and (b) female subjects. Values include individual breaths for all subjects grouped into three categories of tidal, deep and mixed (tidal and deep cycles followed by apnea periods) breathing in three different postures (supine, side and prone).***

4.2.2. *Start time of apnea periods*

Since the purpose of this thesis is to estimate the flow for monitoring the breathing cessations in case of sleep apnea, F_{est} and F_{nasal} signal agreement was assessed by calculating the start time of apnea periods in both signals.

The start time of each breathing cessation in F_{est} and F_{nasal} signal was compared and the absolute value of time differences between them was calculated in milliseconds.

In Figure 31 , an example of F_{est} (dashed line) and F_{nasal} (solid one) signal is illustrated. This figure shows that the start time of apnea periods in F_{est} and F_{nasal} is very close to each other.

Table 3 summarizes the mean value and the standard deviation of absolute value of the time differences for all breathing cessations that happened for all subjects in three different postures.

Considering the results presented in Table 3, the mean value of differences is lower in the supine position in compare with two other positions, so is the standard deviation in this position. As it was expected these values are higher in lateral position than the values in two other positions.

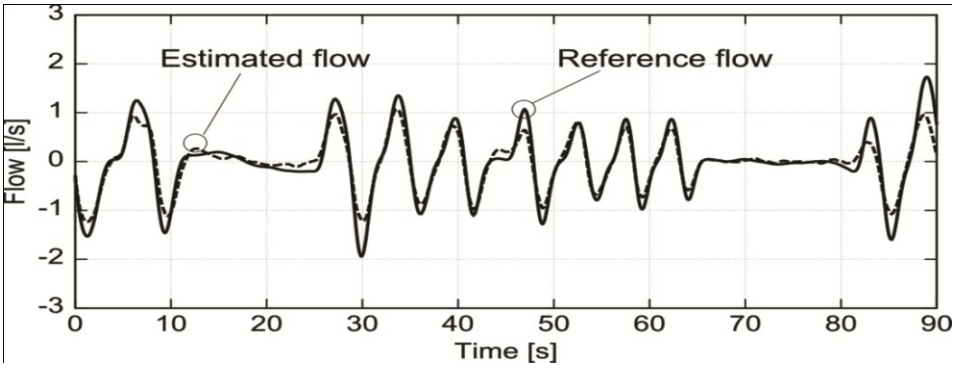

Figure 31. An example of the reference (solid line) and estimated flow (dashed line) with more emphases on the start time of breathing cessation.

Table 3. Mean and standard deviation of absolute value of differences between in the start time of breathing cessation in F_{est} and F_{nasal} for all subjects in three different positions

	Mean	SD
Supine	223(ms)	180
Prone	232(ms)	205
Lateral	291(ms)	230

4.2.3. *Ratio of time at the tidal peak inspiratory flow to the inspiratory time*

In obstructive sleep apnea/hypopnea syndrome (OSAHS), due to partial or complete collapse of pharynx, the flow limitation happens in the upper airway above the thoracic inlet and therefore it is most prominent in inspiration. It gives the inspiration flow measurement very important role in assessing the patients with symptoms suspicious for OSAHS. Ratio of time at the tidal peak inspiratory flow to the inspiratory time (t_{PTIF}/t_I) is one of parameters used for observing inspiratory flow.

In this study, F_{est} and F_{nasal} signal agreement was validated by calculating the t_{PTIF}/t_I ratio as a parameter to assess inspiratory flow. We calculated the t_{PTIF}/t_I ratio for the inspiration phase of each breathing cycle in both estimated (F_{est}) and reference flow (F_{nasal}) signals and compared the values with the Bland-Altman test.

Figure 32 shows the Bland-Altman diagram for t_{PTIF}/t_I ratio extracted from F_{est} and F_{nasal}, for all subjects during tidal breathing in different positions with 95% confidence intervals. Mean values of t_{PTIF}/t_I ratio calculated from the F_{est} and F_{nasal} vs. the difference between t_{PTIF}/t_I ratios from the both signals are depicted separately for each position (supine, prone and lateral).

Table 4 summarizes the mean and the standard deviation of absolute values of the differences between the t_{PTIF}/t_I ratios which is calculated over all breathing cycles from the reference and the estimated flow signals.

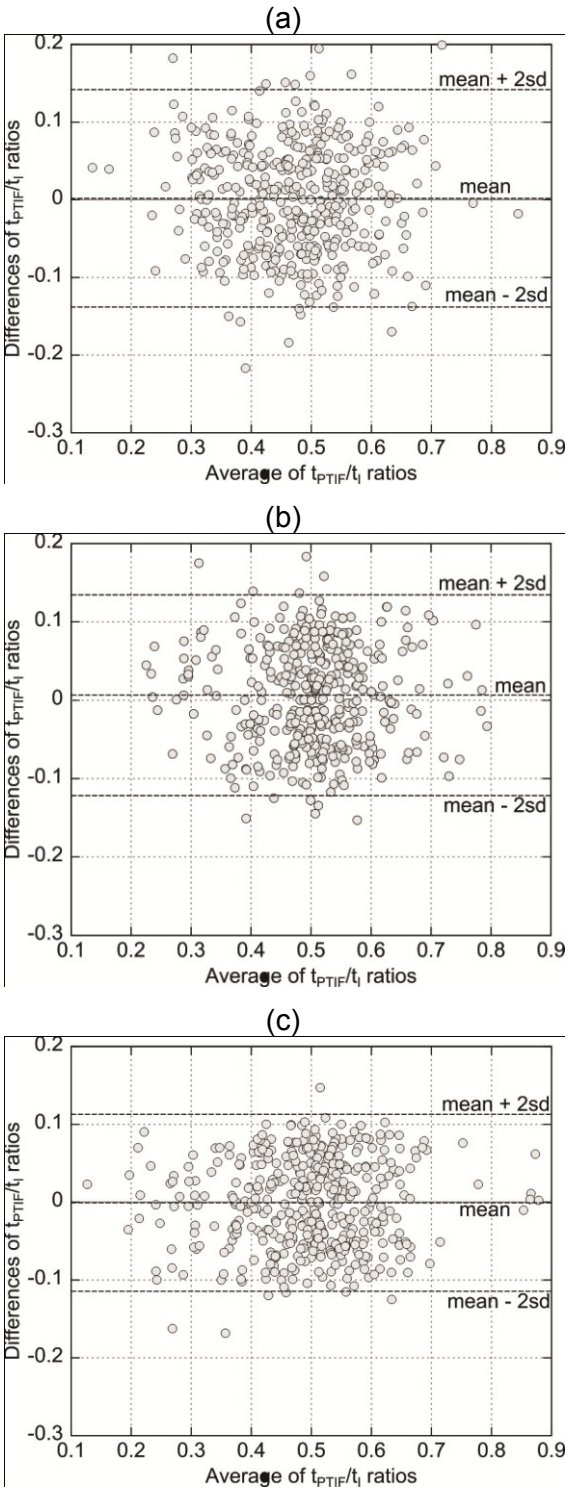

Figure 32. Bland-Altman diagrams presenting the difference between the $t_{PTIF}=t_I$ ratios calculated for every breathing cycle of the actual and the estimated flows versus the mean values of the $t_{PTIF}=t_I$ ratios in (a) supine, (b) prone (c) lateral positions.

Table 4. Mean and standard deviation of absolute value of differences between t_{PTIF}/t_I ratios calculated for every breathing cycle of reference and estimated flow

	Mean	SD
Supine	0.001	0.060
Prone	0.006	0.064
Lateral	0.000	0.056

4.2.4. *Ratio of time at the tidal peak expiration flow to the expiration time*

Expiratory flow measurement is important for monitoring the reduced lung functions in the disorders like asthma or bronchia, where the obstruction happens within the thoracic and therefore is more obvious in expiration. The ratio t_{PTEF}/t_E is used to detect airflow obstruction especially in young children and new born infants (Ent & Grinten, 1998).

In this study, the t_{PTEF}/t_E ratio was calculated for the expiration phase of each breathing cycle of the estimated (F_{est}) and reference (F_{nasal}) flow signals. The values were analysed with Bland-Altman test.

Figure 33 shows the Bland-Altman diagram for t_{PTEF}/t_E ratio extracted from F_{est} and F_{nasal}, for all subjects during tidal breathing in three different positions.

Table 5 summarizes the mean and the standard deviation of absolute values of the differences between the t_{PTEF}/t_E ratios which is calculated over all breathing cycles from the reference and the estimated flow signals.

Table 5. Mean and standard deviation of absolute value of differences between t_{PTEF}/t_E ratios calculated for every breathing cycle of actual and estimated flow

	Mean	SD
Supine	0.043	0.025
Prone	0.058	0.038
Lateral	0.053	0.035

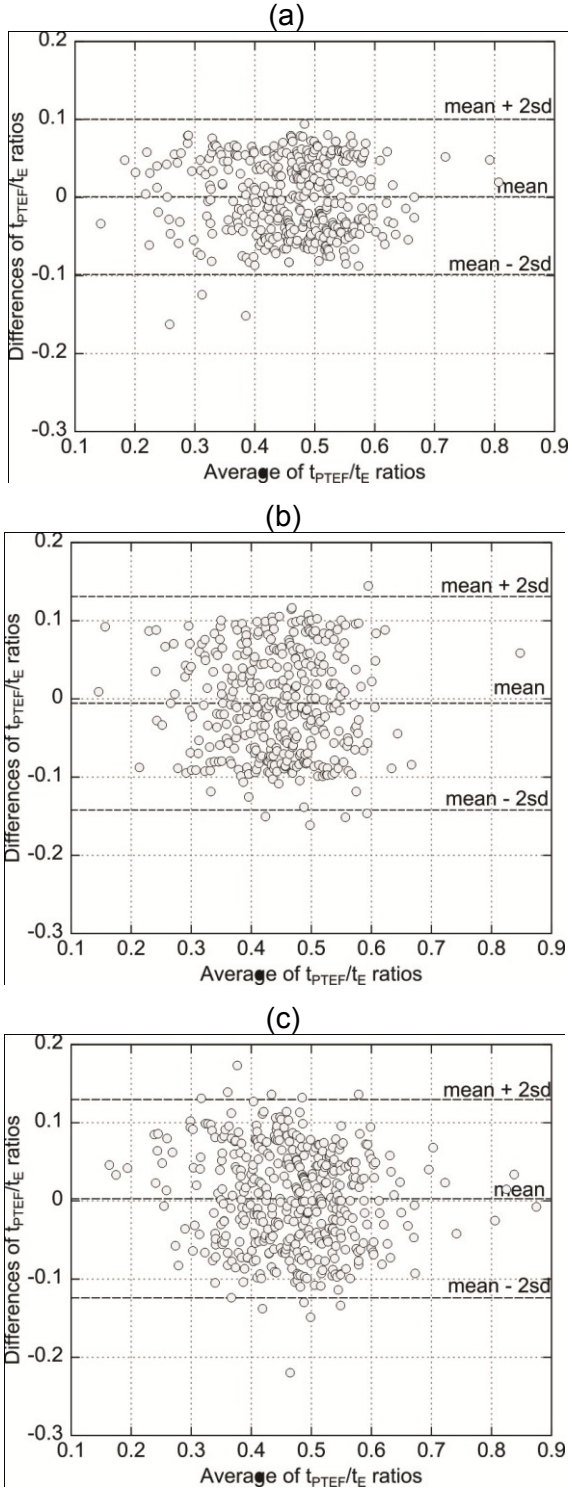

Figure 33. Bland-Altman diagrams presenting the difference between the t_{PTEF}/t_E ratios calculated for every breathing cycle of the actual and the estimated flows versus the mean values of the t_{PTEF}/t_E ratios in (a) supine, (b) prone (c) lateral positions

4.3. Validation of thorax respiratory effort

As the same for flow signal, time domain finite impulse response, neural network and MARS methods were used for estimating the thorax respiratory signal; however the thorax respiratory effort signal was estimated from the acceleration of the rib cage. The committee of experts with the time domain finite impulse response and the neural network models as members minimized the estimation error in respect to the reference thorax effort (V_{Th}) recorded through the thorax belt. This committee was chosen as the final model to estimate the thorax respiratory signal (E_{Th}).

The agreement between the estimated thorax respiratory effort (E_{Th}) and the reference signal (V_{Th}) was assessed by calculating ρ using the equation ***3-2***).

The estimated thorax effort (E_{Th}) and recorded thorax respiratory effort ($V_{Th)}$ signal agreement for each individual measurement is presented in Table 6. In this table, the labels “M” and “F” denote respectively the mate and female subjects. Label “-“ denotes a completely unsuccessful recording.

The entries of Table 6 were summarized as (mean-standard deviation) for men and women in two different diagrams in Figure 34. For women, the value of ρ during the tidal breathing is significantly higher than the ρ values during deep breathing or mix pattern of breathing. This fact is true for three different sleeping positions.

Table 6. Individual agreement between estimated (E_{Th}) and reference thoracic respiratory effort (V_{Th})

S	Gender	Supine			Prone			Lateral		
		Tidal	Deep	Mix	Tidal	Deep	Mix	Tidal	Deep	Mix
1	M	0.9638	0.8689	0.8723	-	0.6548	0.6136	0.6606	0.8621	0.8478
2	M	0.6542	0.8049	0.7766	0.9524	0.9605	0.9588	0.8708	0.8522	0.8407
3	M	0.8323	0.7644	0.8336	0.8144	0.6535	0.6056	0.754	-	0.7588
4	M	0.7279	0.778	0.8054	0.8475	0.8804	0.8695	0.6714	0.8608	0.7873
5	M	0.9029	0.9136	0.8993	0.61	0.7105	0.7237	0.818	0.9185	0.8733
6	M	0.8048	0.8792	0.8818	0.932	0.7784	0.7589	-	0.7611	0.7453
7	M	0.7181	0.7696	0.7606	0.923	0.9444	0.8963	0.7678	0.8489	0.7627
8	M	0.9202	0.9019	0.9092	0.8655	0.929	0.8713	0.9331	0.9114	0.8624
9	M	0.8474	0.8805	0.8524	0.71	0.5562	0.75	0.644	0.5636	-
10	F	0.8964	0.9608	0.9324	0.9008	0.8721	0.8661	0.7399	0.7083	0.7183
11	M	0.8094	0.6961	0.7152	-	0.81	0.92	0.8913	0.8245	0.8568
12	F	0.9092	0.9271	0.9249	0.8419	0.8936	0.8111	0.9462	0.9088	0.8998
13	M	0.9739	0.9649	0.9639	0.6395	0.7201	0.7001	0.7493	0.9389	0.8861
14	M	0.6037	0.9044	0.872	0.9405	0.9661	0.9523	0.81	0.6697	0.5902
15	M	0.7549	0.8382	0.8179	0.68	0.8477	0.8097	-	0.8752	0.8304
16	M	0.6256	0.6757	0.6543	-	0.7521	0.6239	0.7729	0.7737	0.772
17	M	0.8979	0.9555	0.9393	0.75	0.8214	0.86	0.902	0.9349	0.9198
18	F	0.8091	0.9284	0.9108	0.66	0.6911	0.6855	0.7314	0.8522	0.8413
19	M	0.8926	0.933	0.9268	0.688	0.8645	0.7392	0.8608	0.9015	0.8928
20	M	0.6923	0.9053	0.8915	-	-	-	0.8265	0.8597	0.8214

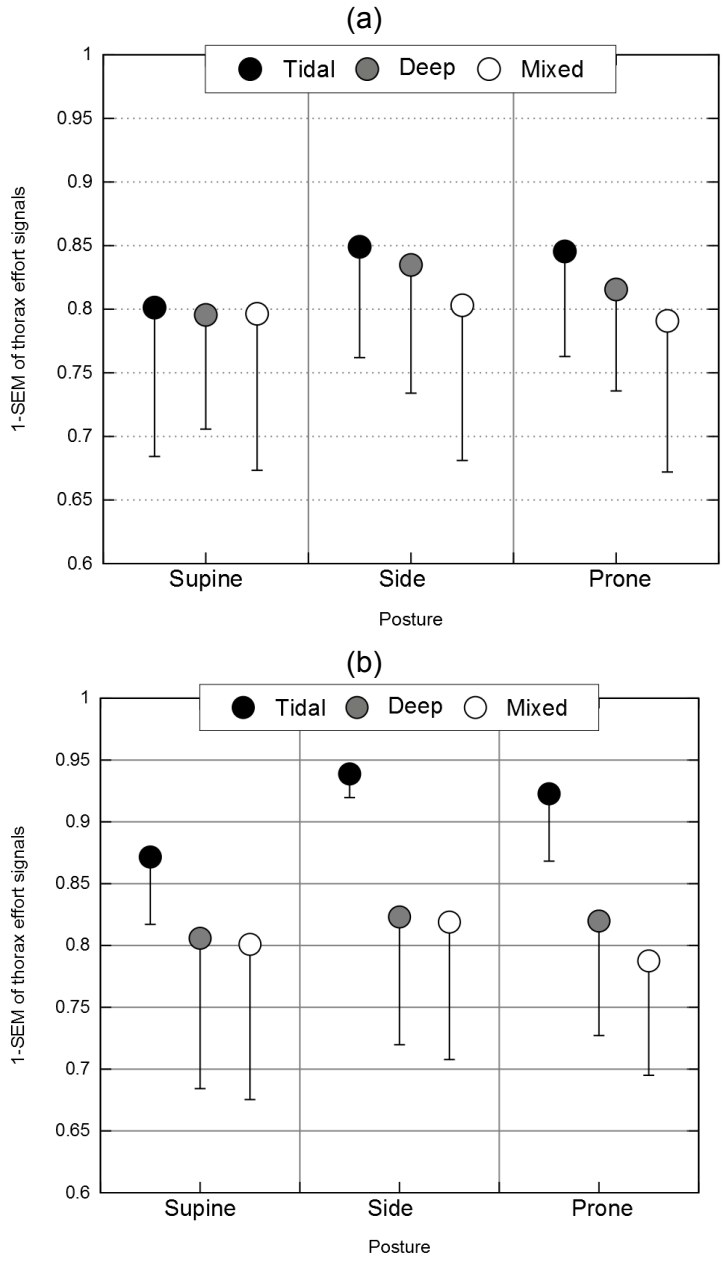

Figure 34. ***Waveform agreement (1-SEM) between E_{Th} and V_{Th} expressed as mean-SD for (a) male subjects and (b) female subjects. Values include individual breaths for all subjects grouped into three categories of tidal, deep and mixed (tidal and deep cycles followed by apnea periods) breathing in three different postures (supine, side and prone).***

4.4. Abdominal respiratory effort agreement

The abdominal respiratory effort was estimated from the acceleration of the abdomen wall. The acceleration signal was recorded by an accelerometer which was mounted on the subjects' belly nearby their umbilicus. For assessment the validity of estimated signal (E_{Abd}), the abdominal effort (V_{Abd}) was simultaneously recorded by a belt fasten around the subjects' abdomen as the reference signal. As the same for flow and thorax respiratory effort signals, time domain finite impulse response, neural network and MARS methods were used as the system identification methods for estimating the abdominal respiratory signal. The committee of experts with the time domain finite impulse response and the neural network models as members minimized the estimation error in respect to the reference abdominal effort (V_{Abd}). This committee was chosen as the final model to estimate the abdominal respiratory signal (E_{Abd}).

The agreement between the estimated abdominal respiratory effort (E_{Abd}) and the reference signal (V_{Abd}) was assessed by calculating ρ using the equation ***3-2***).

Table 7 shows the agreement between estimated abdominal effort (E_{Abd}) and recorded abdominal respiratory effort (V_{Abd}) for all subjects in the three different postures and with the different breathing patterns. In this table "M" and "F" denote the male and female subjects respectively. "-" denotes a completely unsuccessful recording.

These results are summarized in Figure 35 for male and female subjects separately. For women, the value of ρ during the tidal breathing is significantly higher than the ρ values during deep breathing or mix pattern of breathing. This fact is true for three different sleeping positions.

Table 7. Individual agreement between estimated (E_{Abd}) and reference abdominal effort (V_{Abd})

S	Gender	Supine			Prone			Lateral		
		Tidal	Deep	Mix	Tidal	Deep	Mix	Tidal	Deep	Mix
1	M	0.9638	0.8689	0.8723	-	0.6548	0.6136	0.6606	0.8621	0.8478
2	M	0.6542	0.8049	0.7766	0.9524	0.9605	0.9588	0.8708	0.8522	0.8407
3	M	0.8323	0.7644	0.8336	0.8144	0.6535	0.6056	0.754	-	0.7588
4	M	0.7279	0.778	0.8054	0.8475	0.8804	0.8695	0.6714	0.8608	0.7873
5	M	0.9029	0.9136	0.8993	0.61	0.7105	0.7237	0.818	0.9185	0.8733
6	M	0.8048	0.8792	0.8818	0.932	0.7784	0.7589	-	0.7611	0.7453
7	M	0.7181	0.7696	0.7606	0.923	0.9444	0.8963	0.7678	0.8489	0.7627
8	M	0.9202	0.9019	0.9092	0.8655	0.929	0.8713	0.9331	0.9114	0.8624
9	M	0.8474	0.8805	0.8524	0.71	0.5562	0.75	0.644	0.5636	-
10	F	0.8964	0.9608	0.9324	0.9008	0.8721	0.8661	0.7399	0.7083	0.7183
11	M	0.8094	0.6961	0.7152	-	0.81	0.92	0.8913	0.8245	0.8568
12	F	0.9092	0.9271	0.9249	0.8419	0.8936	0.8111	0.9462	0.9088	0.8998
13	M	0.9739	0.9649	0.9639	0.6395	0.7201	0.7001	0.7493	0.9389	0.8861
14	M	0.6037	0.9044	0.872	0.9405	0.9661	0.9523	0.81	0.6697	0.5902
15	M	0.7549	0.8382	0.8179	0.68	0.8477	0.8097	-	0.8752	0.8304
16	M	0.6256	0.6757	0.6543	-	0.7521	0.6239	0.7729	0.7737	0.772
17	M	0.8979	0.9555	0.9393	0.75	0.8214	0.86	0.902	0.9349	0.9198
18	F	0.8091	0.9284	0.9108	0.66	0.6911	0.6855	0.7314	0.8522	0.8413
19	M	0.8926	0.933	0.9268	0.688	0.8645	0.7392	0.8608	0.9015	0.8928
20	M	0.6923	0.9053	0.8915	-	-	-	0.8265	0.8597	0.8214

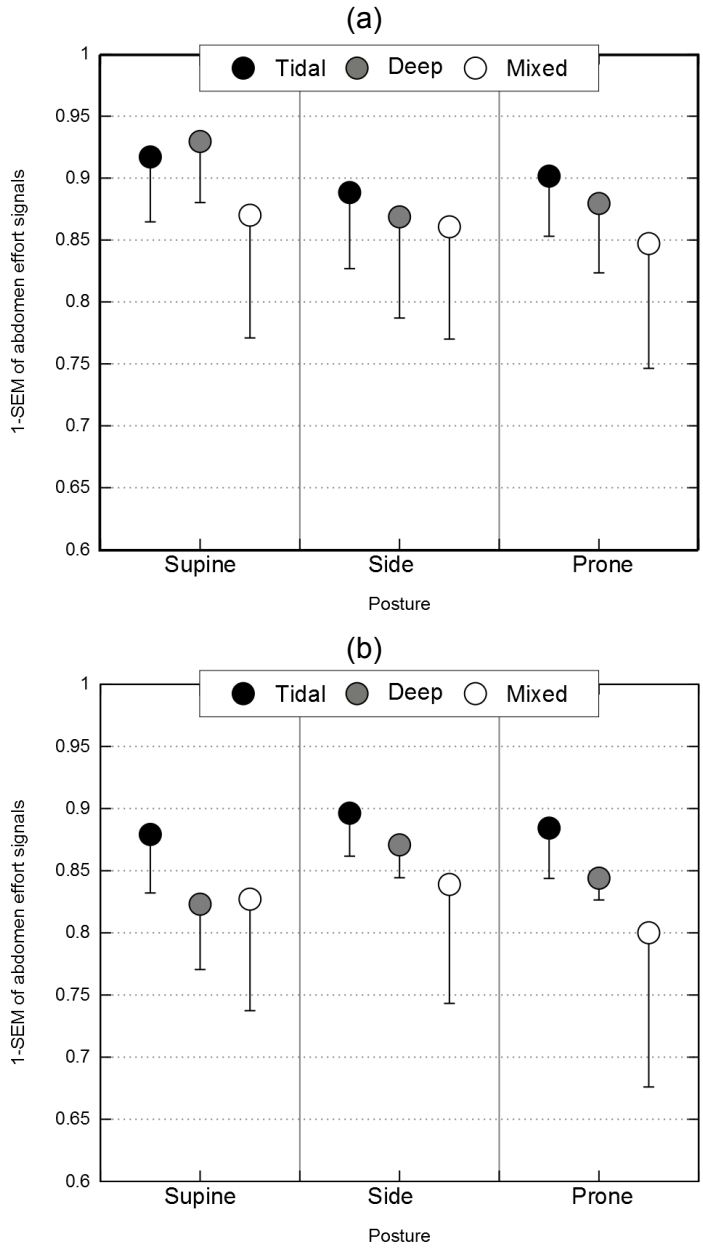

Figure 35. ***Waveform agreement (1-SEM) E_{abd} and V_{abd} expressed as mean-SD for (a) male subjects and (b) female subjects. Values include individual breaths for all subjects grouped into three categories of tidal, deep and mixed (tidal and deep cycles followed by apnea periods) breathing in three different postures (supine, side and prone).***

5. Discussion, Conclusions and Future Works

5.1. Discussion

In this study, we estimated the upper airway flow and the respiratory efforts from acceleration signals recorded from the upper-body by applying machine learning and ensemble learning methodologies.

5.1.1. *Finding an appropriate model structure*

Time domain finite impulse response, neural network and MARSplines methods were used to identify and customize the several models for estimating the flow and the thorax and abdominal respiratory effort signals. Before selecting these methods as the final techniques for estimating the desired signals, several regression and system identification methods such as LASSO (Hastie, Tibshirani, & Friedman, 2009), the Generalized Additive Model(GAM) (Hastie, Tibshirani, & Friedman, 2009) and regression trees (Hastie, Tibshirani, & Friedman, 2009) were investigated.

The motivation for selecting time domain finite impulse response model was its simplicity and accuracy. Selecting the neural network method was inspired by the results of the *Physionet 2010 Computing in Cardiology* challenge where an algorithm using neural networks provided the best results in estimating respiration signals (Rodrigues, 2010). For this study each neural network model was trained and tested five times, and the output was calculated by averaging the five output results.

MARSplines technique was chosen because it does not assume or impose any particular type or class of relationship (e.g., linear, logistic, etc.) between the input variables and the variable of interest (Friedman, 1991). It constructs this relationship from a set of factors that are entirely driven from the regression data. According to our investigation, this particular feature of MARSplines could have been very useful for the

purpose of this thesis where the type of the relationship between the input variables and the variable of interest wasn't obvious and it was very hard to assume any particular type of relationship between them; however the result of applying this method for this study didn't show any significant improvement in estimation error in compare with other methods.

After customizing the several models with three different machine learning methods, we employed an ensemble learning approach to combine the outputs of models, treating them as a committee of experts. The principle of ensemble learning is that the decision of the committee should have better overall accuracy, on average, than any individual committee member (Sammut & Webb, Encyclopedia of Machine Learning, 2010). The committee of experts with the time domain finite impulse response and the neural network models as the members which minimized the estimation error in respect to the reference signals was chosen as the final model to estimate the signals of interest.

The approach was employed in this study for estimating the signals of interest refers as the *black-box* approach (Keesman, 2011). Black-box system identification is a purely data-driven modeling tool without any need to have a first–principles model of the system. At the first step this modeling tool is useful for learning more about the system. But in some cases, it is useful to know about the effect and roll of each input variable in estimating the desired variables. For instance in this study it is very useful to know that the acceleration of suprasternal notch in which direction or plane is more effective in estimating flow.

5.1.2. *Flow estimation and validation*

For estimating the flow, we used the signals recorded from three accelerometers mounted on the suprasternal notch, the thorax and the abdomen of subjects, for three lying positions (supine, lateral and prone) and two different flow rate regimes (tidal and high amplitude breathing). In the study conducted by Morillo et al. (Morillo, Ojeda, Foix, & Jim, 2010) and our previous study (Dehkordi, Marzencki, Tavakolian, Kaminska, & Kaminska, 2011), the respiratory waveform was extracted from the vibration acquired by an accelerometer mounted on the suprasternal notch. We found that using signals recorded by three accelerometers improves the results significantly.

For accessing the validity of the estimated flow, we simultaneously recorded the nasal/oral flow through the nasal cannula connected to a pressure transducer as the reference signal. The parameter ρ for the estimated and reference flow was calculated as defined in equation 3-1. Since the breathing patterns are different for adult men and women, the result of agreement between the estimated and reference flow signal were presented separately for the male and female subjects in Figure 30. However the short number of female subjects in this study didn't give us this opportunity to investigate the differences in breathing pattern in the estimated flow signal for male and female.

We estimated the start time of apnea periods and their duration in both estimated and reference flow signal to compare the time differences. The mean of the overall difference in the start time of apnea periods for all subjects and conditions was calculated as 249 milliseconds with the standard deviation of 210 milliseconds.

Obstructive Sleep Apnea (OSA), as the result of the flow limitation in the upper airway is most noticeable in inspiration. For assessing the inspiration flow, the ratio of time at the tidal peak inspiration flow to the inspiration time (t_{PTIF}/t_I) for each breathing cycle of the estimated and the reference flow signal was calculated. The mean of the overall error was 0.002 with the standard deviation of 0.06.

Besides that, the agreement between the estimated and the actual flow were determined by measuring the ratio of time at the tidal peak expiration flow to the expiration time (t_{PTEF}/t_E). We calculated the t_{PTEF}/t_E ratio for each breathing cycle of the estimated and the reference flow signal. The mean of the overall error was 0.051 with the standard deviation of 0.031.

An estimate of the severity of apnea/hypopnea is calculated by dividing the number of apneas/hypopneas by the number of hours of sleep, giving an apnea/hypopnea index (AHI). Estimating the AHI needs at least two hours of signal monitoring and recording. In this study, because of the short time of data recording (5 minutes for each subject), estimating the AHI doesn't seem valuable. However, observing the estimated and reference flow signal clearly showed that the estimated flow followed the reference flow perfectly in each period of breathing cessation.

Considering the small amount of error for the estimated t_{PTIF}/t_I and t_{PTEF}/t_E ratios and also the start time of apnea, we can suggest that by using the upper body accelerations as proposed in this research, it is feasible to monitor both the upper airway obstruction and also reduced lung function.

5.1.3. *Thoracic respiratory effort estimation and validation*

We estimated the thoracic respiratory effort by using the signals recorded from an accelerometer placed on the left seventh intercostal space of subjects' rib cage.

To find the best location on the thorax for placing the accelerometer, two options were examined. Considering the results presented by Rendon et al. (Rend´on, Ojeda, Foix, Morillo, & Fern´andez, 2007) and by Tavakolian et al. (Tavakolian, Vaseghi, & Kaminska, 2008), we recorded the thorax acceleration from accelerometers mounted on Xiphoid and the left seventh intercostal space simultaneously. After analyzing the signals, the right seventh rib interspace was chosen as minimized the overall estimation error.

For accessing the validity of the estimated thorax respiratory effort, we simultaneously recorded the thorax effort signal as the reference signal through the strain gauge transducer mounted on the belt. The belt was fastened around the thorax of subjects. The parameter ρ for the estimated and reference flow was calculated as defined in equation 3-1.

It has been reported that males have about 20% greater chest expansion than females in normal breathing (Verschakelen & Demedts, 1995). Due to these differences in thoracic movement for men and women during breathing, the calculated ρ for the estimated and reference thoracic respiratory effort was presented separately for both male and female subjects in Figure 34.

5.1.4. *Abdominal respiratory effort estimation and validation*

The abdominal respiration effort was estimated using the signal recorded by an accelerometer mounted on the abdomen wall nearby the subjects' umbilicus. Simultaneously the abdominal respiratory effort was recorded as the reference signal by

the strain gauge transducer mounted on a belt. The belt was fastened around the abdomen of the subjects.

The agreement between the estimated and reference abdominal effort for all subjects and conditions, ρ, was calculated as defined in equation 3-3. The parameter was reported for men and women separately in Figure 35.

According to Figure 35, the mean value of ρ for women during deep breathing is significantly less the mean value of this parameter for men during deep breathing. It may be the outcome of this fact that during deep breathing the women had significantly less abdominal movements than the men (Ragnarsdóttir & Kristinsdóttir, 2006). However because of the short number of women in this study it is not possible to release this finding as the general result.

In this study, during the signal acquisition manoeuvre, the subjects were asked repetitively to hold their breath for more than 10 seconds in order to simulate apnea periods. Since controlled holding of breath is very similar to the lack of respiratory drive, for most subjects, absence of flow was synchronized with the absence of efforts. For some subjects however, the absence of flow in the upper airways was accompanied by some effort in the thorax and the abdomen.

Normal breathing movements are considered to be a combination of abdominal and lower thoracic movements (Chaitlow, Bradley, & Gilbert, 2002). As these movements are three-dimensional, it could be argued that measuring respiratory movements by accelerometer is not sufficient. A result of the study of Moll and Wright (Moll & Wright, 1972) is that they measured chest expansion both circumferentially and diametrically (transverse and anterior-posterior) and after comparing the results they stated that ‘it should be sufficient to measure expansion in one plane only’.

5.2. Conclusion and future work

This study investigates a method of monitoring respiratory parameters using three accelerometers mounted on the torso with special focus on sleep apnea monitoring. The novelty of this research is not in proposing a general methodology of

using accelerometers to quantify respiration, which was done before, but rather to expand this methodology further to capture all required respiratory parameters of flow and efforts, as are registered in PSG, and assess its accuracy in estimating the actual amplitude of the signal rather than only estimating the breath rate. Furthermore, we estimated the t_{PTIF}/t_I and t_{PTEF}/t_E ratios which can be used to monitor both obstruction in the upper airways and reduced lung function. What also distinguishes this research from the prior studies is the use of ensemble learning for processing and analyzing the signals.

The main objective of this study was to introduce an inexpensive and easy to use alternative methodology in monitoring sleep breathing disorders, and more specifically the sleep apnea syndrome, but there has been no intention to suggest this method as a replacement to PSG and comprehensive sleep lab studies.

The results of the paper were obtained from the signals measured in the same session of recording while it would be ideal to further confirm the findings in a multisession and multi-day paradigm as the next step of confirmation. It is intuitive that the same morphology of signals should lead to the same accuracy but the challenge might be more on an accurate re-setup and placement of sensors to obtain the same morphology of tri-axial accelerations. Accuracy of accelerometry-based respiratory signals will also have to be confirmed in a group of older individuals as well as in overweight and obese subjects.

Considering the possibility of recording the torso accelerations using contactless methodologies (Tavakolian, Vaseghi, & Kaminska, 2008), this study can also potentially lead to a contactless monitoring of respiration, resolving situations such as Sudden Infant Death Syndrome (SIDS) where an actual placement of electrodes on the body is cumbersome.

Last but not the least, recent advances in hemodynamic analysis using precordial acceleration signals, recorded from the surface of the torso (Morillo, Ojeda, Foix, & Jim, 2010), (Tavakolian, Blaber, & Ngai, 2010) can provide us with extra tools to also monitor the cardiovascular system in parallel to the monitoring of pulmonary system as proposed in this research. This means that a system based on torso acceleration might be

considered as a very simple and less intrusive methodology for portable monitoring of cardiopulmonary parameters based on the guidelines defined by the American Thoracic Society (Medicine, 2005).

Reference List

Ballester, E., Solans, M., Vila X, X., Hernandez, L., Quintó, L., & Bolivar, I. (2000). Evaluation of a portable respiratory recording device for detecting apnoeas and hypopnoeas in subjects from a general population. *European Respiratory Journal* , 16(1): 123-7.

Bates, A., Ling, M. J., Mann, J., & Arvind, D. K. (2010). Respiratory Rate and Flow Waveform Estimation from Tri-axial Accelerometer. *Body Sensor Networks (BSN)* (pp. 144-150). Singapore: IEEE Conference Publications .

Bates, J., Schmalisch, G., & Stocks, J. (2000). Tidal breath analysis for infant pulmonary function testing. *ERS/ATS Task Force on Standards for infant Respiratory Function Testing, European Respiratory Society/American Thoracic Society. ERS Journals European Respiratory Journal* , 16(6): 1180-92.

Batzel, J. J., Kappel, F., Schneditz, D., & Tran, H. T. (2007). *Cardiovascular and Respiratory Systems: Modeling, Analysis, and Control.* SIAM.

Chaitlow, L., Bradley, D., & Gilbert, C. (2002). *Multidisciplinary Approaches to Breathing Pattern Disorders.* Edinburgh: Churchill Livingston.

Chesson, A. J., Berry, R., & Pack, A. (2003). Practice parameters for the use of portable monitoring devices in the investigation of suspected obstructive sleep apnea in adults. *American Academy of Sleep Medicine; American Thoracic Society; American College of Chest Physicians.Sleep* , 26(7): 907-13.

Collop, N., Anderson, W., Boehlecke, B., Claman, D., Goldberg, R., Gottlieb, D., et al. (2007). Clinical guidelines for the use of unattended portable monitors in the diagnosis of obstructive sleep apnea in adult patients. Portable Monitoring Task Force of the American Academy of Sleep Medicine. *Journal of Clinical Sleep Medicine* , 3(7): 737-47.

Coren, S. (1996). *Sleep Thieves: An Eye-opening Exploration Into the Science and Mysteries of Sleep.* Vancouver: The Free Press.

de Chazal, P., Heneghan, C., Sheridan, E., Reilly, R., Nolan, P., & O'Malley, M. (2003). Automated processing of the single-lead electrocardiogram for the detection of obstructive sleep apnoea. *IEEE Transactions on Information Technology in Biomedicine* , 50: 686--696.

Decker, M. J., Eyal, S., Shinar, Z., Fuxman, Y., Cahan, C., Reeves, W. C., et al. (2010). Validation of ECG-derived sleep architecture and ventilation in sleep apnea and chronic fatigue syndrome. *Sleep and Breathing* , 14(3): 233-239,.

Dehkordi, P., Marzencki, M., Tavakolian, K., Kaminska, M., & Kaminska, B. (2011). Validation of Respiratory Signal Derived from Suprasternal Notch Acceleration for Sleep Apnea Detection. *IEEE Engineering in Medicine and Biology* (pp. 3824 - 3827). Boston, Massachusetts USA: IEEE confrence publication.

Embela systems, I. (2011). *Close to our customers*. Retrieved 03 23, 2012, from Embela: http://www.embla.com/index.cfm/id/14/Closer-to-our-Customers/

Embla systems, I. (2010, 10). *Embletta gold device.* Retrieved 03 23, 2012, from Embla: http://www.embla.com/files/embla//downloads/NewBrochures/GoldLoResFinal.pdf

Ent, C., & Grinten, C. (1998). Time to peak tidal expiratory flow and the neuromuscular control of expiration. *European Respiratory Journal* , 12(3): 646-52.

Ernst, J. M., Litvack, D. A., Lozano, D. L., Cacioppo, J. T., & Berntson, G. G. (1999). Impedance pneumography: noise as signal in impedance cardiography. *Psychophysiology* , 36: 333-338.

Friedman, J. H. (1991). Multivariate Adaptive Regression Splines (with discussion). *Annals of Statistics* , 19:1-141.

Gilbert, R., Auchincloss, J. J., Brodsky, J., & Boden, W. (1972). Changes in tidal volume, frequency, and ventilation induced by their measurement. *Journal of Applied Physiology* , 33: 252-4.

Gubbi, J., & Khandoker, A. (2012). Classification of sleep apnea types using wavelet packet analysis of short-term ECG signals. *Journal of Clinical Monitoring and Computing,* , 26: 1-11.

Hastie, T., Tibshirani, R., & Friedman, J. (2009). *The Elements of Statistical Learning:Data Mining, Inference, and Prediction.* New york: Springer.

Hastie, T., Tibshirani, R., & Friedman, J. (2009). *The Elements of Statistical Learning:Data Mining, Inference, and Prediction.* New york: Springer.

Houtveen, J. H., Groot, P. F., & de Geus, E. J. (2006). Validation of the thoracic impedance derived respiratory signal using multilevel analysis. *International Journal of Psychophysiology* , 56: 97--106.

Javaheri, S., Parker, T., & Wexler, L. (1995). Occult sleep-disordered breathing in stable congestive heart failure. *Annals of Internal Medicine* , 122: 487-492.

Keesman, K. J. (2011). *System identification, an introduction.* London: Springer.

Kushida, C., Littner, M., & Morgenthaler, T. (2005). Practice parameters for the indications for polysomnography and related procedures: An update for 2005. *Sleep* , 28 (4): 499–519.

Malhotra, A., & Owens, R. L. (2010). What Is Central Sleep Apnea? *Respiratory care* , 55(9):1168–1176.

Malhotra, A., & White, D. (2002). Obstructive sleep apnoea. *Lancet* , 360(9328):237-45.

Malmivou, J., & Plonsey, R. (1995). *Bioelectromagnetism.* New york: Oxford university press.

Mathworks. (2011). *System Identification Toolbox* . Retrieved 01 01, 2012, from Mathworks: http://www.mathworks.com/products/sysid/

Mazeika, G. G., & Swanson, R. (2007). An Introduction to Respiratory Inductance Plethysmography. *Pro-Tech Services, Inc.*

McNicholas, W., & Lévy, P. (2011). Portable monitoring in sleep apnoea: the way forward? *European Respiratory Journal* , 37: 749–751.

Medicine, A. A. (2005). International Classification of Sleep Disorders. *Rochester American Academy of Sleep Medicine* .

Mendez, M. O., Corthout, J., Huffel, S. V., Matteucci, M., Penzel, T., Cerutti, S., et al. (2010). Automatic screening of obstructive sleep apnea from the ECG based on empirical mode decomposition and wavelet analysis. *IOP PUBLISHING* , 31: 273–289.

Moll, J., & Wright, W. (1972). An objective clinical study of chest expansion. *Annals of the Rheumatic Diseases* , 31:1–8.

Moody, G. B., Mark, R. G., Bump, M., Weinstein, J. S., Aaron D., B., Mietus, J. E., et al. (1986). Clinical validation of the ECG-derived respiration (EDR) technique. *Computers in Cardiology* (pp. 13: 507-510). Washington, DC: IEEE Computer Society Press.

Moody, G. B., Mark, R. G., Zocco, A., & Mantero, S. (1985). Derivation of Respiratory Signals from Multi-lead ECGs. *Computers in Cardiology* , 12: 113-116.

Morillo, D. S., Ojeda, j. L., Foix, L. F., & Jim, A. L. (2010). An Accelerometer-Based Device for Sleep Apnea Screening. *IEEE Transaction on biomedical engineering* , 14(491--499).

Nabili, S. T., & Verneuil, A. (2004, 04 23). *Sleep apnea*. Retrieved 1 14, 2012, from MedicineNet.com: http://www.medicinenet.com/sleep_apnea/article.htm

Nayak, R., Jain, L., & Ting, B. (2001). ARTIFICIAL NEURAL NETWORKS IN BIOMEDICAL. *School of Computer and Information Science* .

Penzel, T., McNames, J., Murray, A., P., d. C., Moody, G., & B., R. (2002). Systematic comparison of different algorithms for apnoea detection based on electrocardiogram recording. *Medical & Biological Engineering & Computing* , 402-7.

Phan, D. H., Bonnet, S., Guillemaud, R., & Castelli, E. (2008). Estimation of respiratory waveform using an accelerometer. *IEEE International Symposium on Biomedical Engineering* (pp. 1493 - 1496). Paris, France.: IEEE conference publication.

PORTIER, F., & PORTMANN, A. e. (2000). Evaluation of Home versus Laboratory Polysomnography in the Diagnosis of Sleep Apnea Syndrome. *American Journal of Respiratory and Critical Care Medicine* , 169(3): 814-818 .

Public Health Agency of Canada, p. (2007, 11 22). *Sleep Apnea*. Retrieved 04 01, 2012, from Public Health Agency of Canada: http://www.phac-aspc.gc.ca/publicat/2007/lbrdc-vsmrc/sleep-sommeil-eng.php

Que, C.-L., Kolmaga, C., Durand, L.-G., Kelly, S., & Macklem, P. T. (2002). Phonospirometry for noninvasive measurement of ventilation: methodology and preliminary results. *Journal of Applied Physiology* , 93: 1515--1526.

Ragnarsdóttir, M., & Kristinsdóttir, E. K. (2006). Breathing movements and breathing patterns among healthy men and women 20–69 years of age. *respiration* , 73:48–54.

Randerath, W. J., Sanner, B. M., & Somers, V. K. (2006). *Sleep Apnea: Current Diagnosis And Treatment (Progress in Respiratory Research).* Berlin: S Karger Pub.

Rapoport, D., Norman, R., & Nielson, M. (2001). An introduction to Nasal Pressure Airflow Measurement. *Pro-Tech Services, Inc* .

Reinvuo, T., Hannula, M., Sorvoja, H., & Alasaa, E. (2006). Measurement of respiratory rate with high-resolution accelerometer and emfit pressure sensor. *IEEE Sensors Applications Symposium* (pp. 192-195). Houston, Texas USA: IEEE conferences publication.

Rend´on, D. B., Ojeda, J. L., Foix, L. F., Morillo, D. S., & Fern´andez, ,. M. (2007). Mapping the human body for vibrations using an accelerometer. *IEEE Engineering in Medicine and Biology conference* (pp. 1671–1674.). Lyon: IEEE conference publication.

Rodrigues, R. (2010). Filling in the Gap: a General Method using Neural Networks. *Computing in Cardiology*, (pp. 453 - 456). Belfast.

Sammut, C., & Webb, G. I. (2010). *Encyclopedia of Machine Learning.* New york: Springer.

Sammut, C., & Webb, G. I. (2010). *Encyclopedia of Machine Learning.* New york: Springer.

Savitzky, A., & Golay, M. J. (1964). Smoothing and Differentiation of Data by Simplified Least Squares Procedures. *Analytical Chemistry* , 36(8): 1627–1639.

Seppa, V., Viik, J., & Hyttinen, J. (2010). Assessment of Pulmonary Flow Using Impedance Pneumography. *IEEE Transactions on Information Technology in Biomedicine* , 57: 2277-2285.

Stocks, J., Sly, P. D., Tepper, R. S., & Morgan, W. J. (1996). *Infant Respiratory Function Testing.* Wiley-Liss.

Tarrant, S., Ellis, R., Flack, F., & Selley, W. (1997). Comparative review of techniques for recording respiratory events at rest and during deglutition. *Dysphagia.* , 12: 24-38.

Tavakolian, K., Blaber, A., & Ngai, B. &. (2010). Estimation of hemodynamic parameters from Seismocardiogram. *Computing in Cardiology* (pp. 1055-1058). Belfast: Computing in Cardiology .

Tavakolian, K., Vaseghi, A., & Kaminska, B. (2008). Improvement of ballistocardiogram processing by inclusion of respiration information. *Physiological measurement* , 29(771-81).

Verschakelen, J., & Demedts, M. (1995). Normal thoracoabdominal motions: Influence of sex, age, posture and breath size. *American Journal of Respiratory and Critical Care Medicine* , 151:399–405.

Whittle, A., Finch, S., Mortimore, I., MacKay, T., & Douglas, N. (1997). Use of home sleep studies for diagnosis of the sleep apnoea/hypopnoea syndrome. *Thorax* , 52(12):1068-73.

Yadollahi, A., & Mousavi, Z. (2006). A Robust Method for Heart Sound Localization using Lung Sounds Entropy. *IEEE Transactions on Biomedical Engineering* , 53(3): 497-502.

Yadollahi, A., & Moussavi, Z. (2010). Sleep apnea monitoring and diagnosis based on tracheal respiratory sounds and pulse oximetery. *Medical & Biological Engineering & Computing* , 48(11): 1087-97.

Yap, Y. L., & Moussavi, Z. (2002). Acoustic airflow estimation from tracheal sound power. *IEEE Canadian Conference on Electrical and Computer Engineering, 2002* (pp. 1073-1076). Winnipeg, Manitoba, Canada: IEEE conference publications.

Young, T., Peppard, P., & Gottlieb, D. (2002). American Journal of Respiratory and Critical Care Medicine. *Epidemiology of obstructive sleep apnea: a population health perspective* , 1217–39.

Appendices

Appendix A.

Experiment protocol for signal acquisition

1. Examiner prepares the test setup, as presented in section 3.2.2.Test Setup.
2. Examiner activates the PC and the Ni DAQ USB acquisition system.
3. Examiner starts LabVIEW on the laptop PC and runs a custom built LabVIEW Virtual Instrument (VI) for performing the data saving.
4. Examiner introduces the set material and explains safety rules to subjects.
5. Examiner introduces the breathing pattern to subjects.
6. Examiner asks the subject to expose his chest.
7. Examiner puts 4 pre-gelled electrodes on subject's right clavicle, left clavicle, last left rib and last right rib.
8. Examiner connects strain gauge transducers to belts.
9. Examiner fastens the first belt around the subject's thorax.
10. Examiner fastens another belt around the subject's abdomen.
11. Examiner positions the nasal/oral cannula on the subject and place the cannula sensor tips into the subject's nostrils and in front of the mouth as illustrated in (b)
12. Once the nasal/oral prongs are comfortably placed, examiner slides the cannula tubing over the subject's ears and down the front of chest.
13. Examiner asks the subject to lie supine on the bed.
14. Examiner attaches ECG cables to ECG electrodes following the indications on the cable. The left leg (LL) cable is left disconnected.
15. Examiner cuts three 1cm x 1cm pieces of double sided tape.
16. Using three 1cm x 1 cm piece of double sided tape, examiner fixes the MEMS accelerometer on subject on suprasternal notch, the left seventh rib interspace and abdomen one by one. Examiner can use paper tape to make the accelerometers more stable.
17. Examiner connects the nasal/oral cannula connectors to the nasal/oral input of pressure transducer.
18. Examiner activates the ECG machine, the accelerometer amplifier, and the biopac data acquisition system.
19. Examiner asks the subject to breathe normally according the introduced breathing pattern but remain motionless and quiet for several minutes.
20. By running the Labview VI, data recording starts. Examiner saves each subject's data in separate files, labeling them in the following way:
21. [SubjectName][SubjectPosition]TrainingSet.lis
22. Examiner stops Labview VI after acquiring 120s worth of data.
23. Examiner asks the subject to take a short rest.

24. Examiner asks the subject to breathe according the introduced breathing pattern but remain motionless and quiet for several minutes.
25. Examiner activates the Labview data acquisition VI to start data recording. A file is chosen to save new data, labeling it as [SubjectName][SubjectPosition]TestSet.lis.
26. Examiner stops Labview VI after acquiring 120s worth of data.
27. Examiner asks the subject to change his position to left side. The steps from 19-25 repeats.
28. Examiner asks the subject to change his position to prone. The steps from 19-25 repeats.
29. Examiner detaches Pressure Sensor Cannula.
30. Examiner detaches the accelerometers and ECG cables from the subject and asks the subject to stand up.
31. Examiner opens the belts and carefully removes the ECG electrodes from the subject.

Appendix B

List of materials

Materials which have been used for data acquisition in this study in CiBER lab are listed in table below.

List of material used in data acquisition process

	Item	Quantity
1	Ni DAQ USB acquisition system with NI 9205 module, USB cable and power supply	1
2	Biopac MP100A-CE data acquisition system	1
3	Biopac UIM100C	2
4	Biopac 12V power supply	1
5	Biopack Strain gauge transducer	2
6	Belt	2
7	ADXL335z tri-axis MEMS accelerometer	3
8	Braebon Pressure Transducer Airflow System 0580D	1
9	Braebon Keyhole to 3.5mm Male Phone 0353	1
10	Braebon Nasal & oral cannula & safety filter 0589	1
11	Nihon Kohden ECG machine	1
12	Set of cables for the ECG machine	1
13	Power cable for the ECG machine	1
14	ECG Pregelled Electrodes	3
15	Double sided tape	1
16	Paper tape	1
17	Bed	1
18	Jack audio cable	2
19	BNC cable with crocodile connectors	1
21	Rigid wires for signal connection to the DAQ card	5
22	A personal computer running a custom built LabVIEW Virtual Instrument (VI)	1

Appendix C.

Calibrating the Airflow Pressure Sensor

The airflow pressure sensor used in this study is a qualitative pressure sensor designed to measure nasal/oral pressure associated with human respiratory activity. For obtaining quantitative data from this sensor, it was calibrated with a water manometer as describe below:

Connected the pressure sensor to the water manometer.

Using a manometer, applied a known pressure.

Set a corresponding voltage for the known pressure.

Repeated steps 2 and 3 for 5 inputs.

Table below shows the applied pressure and corresponding voltage.

Applied pressure to airflow pressure sensor and corresponding voltage

	Applied Pressure(cmH_2O)	Corresponding Voltage(V)
1	-10	-1.91
2	-6	-1.250
3	0	-0.038
4	6	1.3
5	10	1.90

Calibration information:

- Slop: 5.250(cmH_2O)/V
- Intercept: 0.026 cmH_2O

Appendix D.

Publications

Journal paper

Parastoo Dehkordi, Marcin Marzencki, Kouhyar Tavakolian, Marta Kaminska & Bozena Kaminska (2012). Assessment of Respiratory Flow and Efforts Using Upper-Body Accelerations Considering the Sleep Apnea Syndrome. Submitted to IEEE Transactions on Biomedical Engineering.

Conference papers

Parastoo Dehkordi, Marcin Marzencki, Kouhyar Tavakolian, Marta Kaminska & Bozena Kaminska (2011). Validation of Respiratory Signal Derived from Suprasternal Notch Acceleration for Sleep Apnea Detection. IEEE Engineering in Medicine and Biology (pp. 3824 - 3827). Boston, Massachusetts USA: IEEE confrence publication.

Parastoo Dehkordi, Marcin Marzencki, Kouhyar Tavakolian, Marta Kaminska & Bozena Kaminska (2012). Monitoring Torso Acceleration for Estimating Respiratory Flow and Efforts for Sleep Apnea Detection and Classification. Accepted to IEEE Engineering Conference in Medicine and Biology. *San Diego, California USA*.